Solid Oxide Fuel Cell/Gas Turbine Hybrid System Studies

Sanchit Gupta

Delft University of Technology

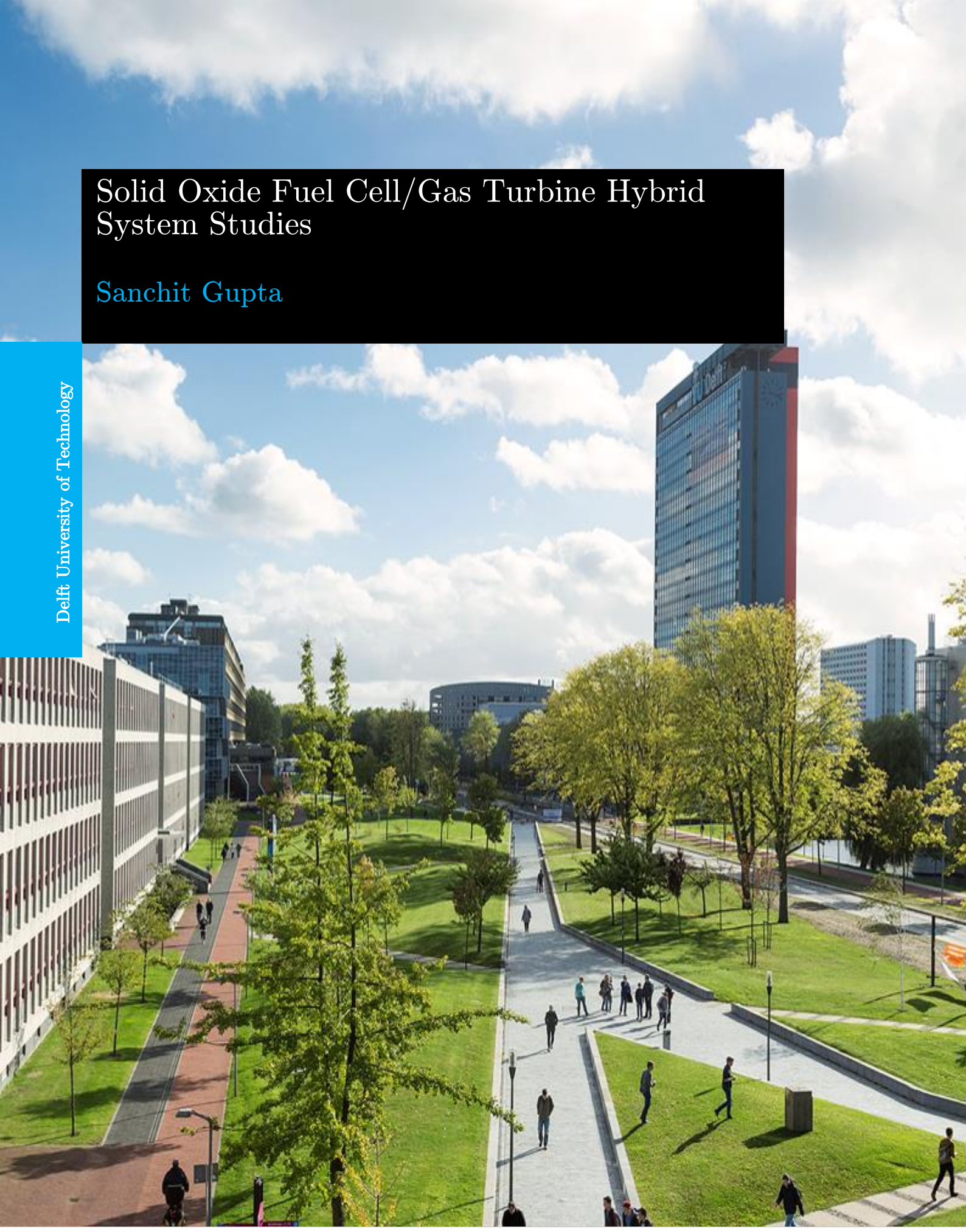

TU Delft Delft University of Technology

Challenge the future

Solid Oxide Fuel Cell/Gas Turbine Hybrid System Studies

Master of Science Thesis

By

Sanchit Gupta

MSc Sustainable Energy Technology
Delft University of Technology

Supervisors

Dr. Hrishikesh Patel, TU Delft
Dr. P.V. Aravind, TU Delft
Ir. Theo Woudstra, TU Delft

2017

TU Delft Delft University of Technology

Abstract

Power generation systems based on SOFCs provide a highly efficient alternative to traditional systems. In the present study a sensitivity analysis with cell operating temperature, pressure ratio and fuel utilization as system parameters is performed on a SOFC-GT system fed by Hydrogen and Methane. Exergy losses in different system components and their dependence on system operating parameters and fuel chemistry are investigated in detail. In the considered ranges system efficiency increased with both cell operating temperature and fuel utilization. A flat optimum with pressure ratio was found for Hydrogen (2.5) and Methane (5). The main causes of high losses in the system are found to be very different for Hydrogen and Methane which leads to different optimization strategies. Following the optimizations comparable system exergy efficiencies were obtained with Hydrogen (76.2%) and Methane (78%). Electrical efficiencies were 74.6% and 80.9% with Hydrogen and Methane respectively. An additional study of a SOFC system without a gas turbine was also undertaken with 4 fuels (Methane, Hydrogen, Methanol and Ammonia). It was observed that it is possible to achieve a high system efficiency by minimizing the excess heat left due to the removal of the gas turbine and utilizing it completely for internal reforming of the fuel. An electrical efficiency of 73.3% was achieved with Methane without the gas turbine.

Acknowledgements

I would like to express my sincere gratitude to all those without whom this work would not have been possible. Firstly I thank Dr. P.V. Aravind for giving me the opportunity for working on this assignment and guiding me. I would like to thank my daily supervisor Dr. H.C. Patel for his guidance and help throughout. Special thanks to Ir. Theo Woudstra for his supervision, the lengthy and excellent discussions and for lending all the possible support especially towards the end. I would like to thank my family for providing the emotional support and motivation till the very end. I would also like to thank my friends Yash, Raunak, Jorge and Suvarna (among others) for helping me out when I needed it the most.

Contents

List of Figures

List of Tables

Nomenclature

Subscripts

el	Electrical
ex	Exergy
chem	Chemical
nst	Nernst
phy	Physical
rev	Reversible
thm	Thermomechanical

Abbreviations

ASR	Area Specific Resistance
CB	Combustor
CP	Compressor
FC	Fuel Cell
GT	Gas Turbine
HX	Heat Exchanger
SOFC	Solid Oxide Fuel Cell
ST	Stack

Symbols

η	Efficiency

1

Introduction

Power generation systems based on Solid Oxide Fuel Cells (SOFCs) have been recognized as a promising future power source [1]. High power generation efficiency, fuel flexibility and ultra-low emissions from SOFCs are their main advantages [2]. Another major advantage of SOFCs is their ability to be combined with other systems resulting in creation of hybrid systems with even higher efficiency [3]. It can be combined with many different thermodynamic cycles to obtain systems with very high efficiencies [4]. The high grade heat available at their exhaust can be used to drive a steam cycle or Gas Turbine (GT) cycle to utilize the unused heat and fuel leading to the creation of a more efficient system [4-7]. The high operating temperature and the presence of a catalyst that allows internal reforming of certain fuels, make it possible to use a variety of fuels such as methanol, methane, ammonia etc. to be used in an SOFC. There are many studies available regarding the usage of SOFCs with these fuels [8-14]. However it is still unclear which fuel would be the most suitable energy carrier in the future.

Biomass has the potential to become a sustainable energy source. However burning raw biomass to produce energy is not very efficient or environmentally friendly, moreover biomass is available in various different forms such as crops, residues, municipal waste, wood chips and even algae [15, 16]. This makes direct use of biomass for power production rather problematic [17, 18] and therefore the current focus of development of biomass as an energy source has shifted to conversion of raw biomass into more energy dense forms (such as those mentioned above) which offer better transportability, storage and facilitate efficient use.

1.1. Literature Review

Numerous studies have been conducted on integrated Solid Oxide Fuel Cell - Gas Turbine (SOFC-GT) systems and have been focused on optimization of the system or individual components for particular fuels, identifying sources of exergy losses or considering different system configurations [7, 19-29]. A study also suggested that high efficiencies of up to 80% can be achieved in large scale power plants using SOFC-GT systems [30]. Sucipta et al [27] studied the impact of variation of fuel composition (methane with varying concentrations of H_2, CO_2, H_2O, N_2).

Leucht et al [31] developed a dynamic model of a pressurized SOFC system for application in SOFC/GT hybrid system. Comparison of alternative system configurations revealed that pressurized operation of the SOFC is preferable. Kuchonthara et al [19] compared the effect of steam and recuperation against only heat recuperation in an SOFC/GT system fueled by Hydrogen and concluded that addition of steam recuperation leads to higher system efficiency and specific power. Yi et al [32] studied a SOFC/GT system fueled by Natural Gas with intercooled compression and reported an electrical efficiency of 75.8% (net AC, based on LHV). The influence of using fuel cell stacks in series on fuel cell efficiency alone as well as on system efficiency was studied by Selimovic et al [33]. It was concluded that networked fuel cell stacks lead to a significant increase in system efficiency due to better thermal management. Sarmah et al [34] studied the energetic and exergetic performance of SOFC – Steam cycle hybrid systems. A comparison was made between three different bottoming steam cycles and a maximum exergy efficiency of 54.84% with single pressure steam cycle was obtained.

Traditionally the exergy criterion for SOFC-GT hybrid systems has not been considered by many researchers, however in recent years an increasing number of such studies can be found. Aravind et al [35] evaluated a small scale biomass gasifier – SOFC/GT hybrid system. It was concluded that electrical efficiencies of 54% are achievable and pressure ratio in the range of 4.5 to 7 has a negligible impact on system efficiency. Calise et al [36] performed an exergy analysis of a hybrid SOFC/GT system fueled by Methane and found out that the biggest loss making component is the fuel cell followed by the combustor. Electrical efficiency close to 60% was reported. Granovski et al [30] studied an SOFC/GT system with internal reforming of Methane and reported efficiencies of 70-80%. In another study, energy and exergy analysis were performed on a Methane fueled SOFC/GT system and a sensitivity study with respect to parameters such as fuel flow rate, air flow rate, temperature and pressure was done [37]. Energy and exergy efficiencies of 65.62% and 59.32% respectively were reported. Motahar et al [25] performed an exergy based analysis of an SOFC/GT hybrid system retrofitted with steam injection. Steam injection was found to increase the system exergy efficiency by about 7% to a final value of 65.34% due to a reduction in stack losses. An internal reforming SOFC/GT system integrated with a Rankine bottoming cycle was studied by Mehdi et al [38]. A multi-objective optimization minimizing total cost while maximizing exergy efficiency of the system was performed. Total exergy and net electrical efficiencies of 65.11% and 66.86% were achieved. Haseli et al [24] studied the influence of turbine inlet temperature and compressor pressure ratio on system efficiency, with a Methane fueled SOFC-GT system. At an optimum pressure ratio of 4, maximum thermal efficiency of 60.6% was achieved.

An SOFC/GT system fueled by Methane and Ethanol with external steam reforming was studied by Douvartzides et. al. using the exergy criterion [39]. The stack and after-burner

were found to be the major sources of exergy destruction and system efficiency was higher with Methane as compared to Ethanol.

In a recent study of SOFC-GT systems by Patel et al [40] , 5 different fuels were compared at a particular operating condition. Exergy efficiencies of 75.5% and 70.4% were reported with Methane and Hydrogen respectively. It was found that at the system level the overall efficiency is guided not just by the fuel cell efficiency but also by the heat effects which determine flow distributions throughout the system. Based on an analysis of exergy loss distributions with different fuels it was concluded that the system design needs to be optimized for each individual fuel.

1.2. Thesis Objective and Outline

SOFC-GT systems have been the focus of several studies (with various fuel choices), with some based on exergy analysis as well. However, the studies done so far have dealt with different system configurations, input parameters (therefore different constraints) and with different fuels. Although these studies provide important information regarding the potential of different systems and their optimum operating points, it is difficult to combine the results and optimization strategies in order to draw any conclusions as to which fuel can give the highest efficiency and with which system configuration. No study so far has attempted to optimize the system design for different fuels individually and compare the efficiencies obtained.

It is important therefore, to start with a simple base case model (same configuration and constraints), identify various loss making components along with their dependence on the nature of the fuel in order to optimize the systems for the fuels individually. An attempt can then be made to conclude which fuel presents a better choice (w.r.t electrical efficiency) and with which system configuration. Such a study can bring clarity as to which fuel could be considered as the energy carrier in the future, especially with respect to SOFC-GT systems.

As far as the fuel cell itself is considered, Hydrogen is the most natural fuel since the basic reaction in most of the fuel cells is Hydrogen oxidation, while Methane has been the most investigated fuel in SOFC system studies. If the heat of reforming is considered for different fuels Hydrogen and Methane represent two extreme ends of the spectrum. For Methane the heat of reforming is highest (per mole of Hydrogen produced along with water-gas shift reaction) while for Hydrogen it is absent. Therefore studying in detail the influence of these two fuels on system thermodynamics will help us draw conclusions for other fuels considered with SOFC-GT systems (such as Methanol, Ethanol, Ammonia) that lie somewhere in between the two on the spectrum.

In pursuit of highest system efficiencies the current trend of research on SOFC systems is found to be towards systems with higher complexity [3, 7, 34, 41, 42]. However it has not

been comprehensively studied whether such highly complex systems are indeed necessary to achieve high system efficiencies (electrical). Hence there is a need for a thermodynamic study of an SOFC system without any bottoming cycle to determine the extent of the decrease in efficiency and optimization strategies needed to achieve acceptable efficiencies (with different fuels), if at all they can be achieved. As an indicative study additional fuels (Ammonia and Methanol) are also considered since these fuels have been studied more in SOFC system studies as compared to Hydrogen.

The main objectives of the thesis are as follows –

- Perform a sensitivity analysis on the base configuration with Cell Temperature, Pressure Ratio and Fuel Utilization as parameters, determine optimum values (if any) and quantify the influence of the nature of the fuel on system thermodynamics
- Optimize the system configuration for each fuel using the results of the sensitivity analysis
- Develop and optimize a system without the gas turbine with Hydrogen, Methane, Ammonia and Methanol as fuels

In chapter 2 the theoretical background necessary to understand the working of SOFCs along with the concepts of exergy analysis and carbon deposition are presented. Underlying assumptions and rules for thermodynamic calculations are also highlighted in this chapter. Chapter 3 presents the sensitivity analysis results for the base configuration and discusses the key differences between the results for both the fuels. Using the results from the sensitivity analysis, system optimization is discussed in Chapter 4. Chapter 5 deals with system modeling and optimization for the case without a gas turbine. Conclusions and scope for future work are highlighted in Chapter 6.

2

Theoretical Background

This chapter provides a description of the basic thermodynamic and electrochemical principles involved in the working of SOFCs. A detailed treatment is skipped and the interested reader is referred to [43]. Fundamentals of system exergy analysis are also provided followed by a description of Carbon Deposition and relevant calculation rules in the system modeling software Cycle Tempo.

2.1. SOFC Electrochemistry

A solid oxide fuel cell (SOFC) is an energy conversion device that converts the chemical energy of a fuel into electrical energy without any intermediate thermal or mechanical processes. Equation (2.1) shows the overall chemical reaction involved in a SOFC operating on Hydrogen as the fuel

$$H_2 + \frac{1}{2}O_2 \leftrightarrow H_2O \tag{2.1}$$

This redox reaction is divided into two half-cell reactions namely, Hydrogen oxidation reaction (HOR) and Oxygen reduction reaction (ORR) which take place at the anode and cathode respectively.

$$H_2 + O^{2-} \leftrightarrow H_2O + 2e^- \tag{2.2}$$

$$\frac{1}{2}O_2 + 2e^- \leftrightarrow O^{2-} \tag{2.3}$$

Electrons are released at the anode from where they flow towards the cathode through an external circuit, while oxide ions produced at the cathode flow towards the anode through the electrolyte. The anode is typically made up of Nickel (Ni) / Yttria Stabilized Zirconia (YSZ), the electrolyte which needs to be an electronic insulator is made up of dense YSZ while the cathode material is a composite of YSZ and Strontium doped Lanthanum Manganite (LSM). Figure 1 below depicts the transport processes involved in the functioning of an SOFC.

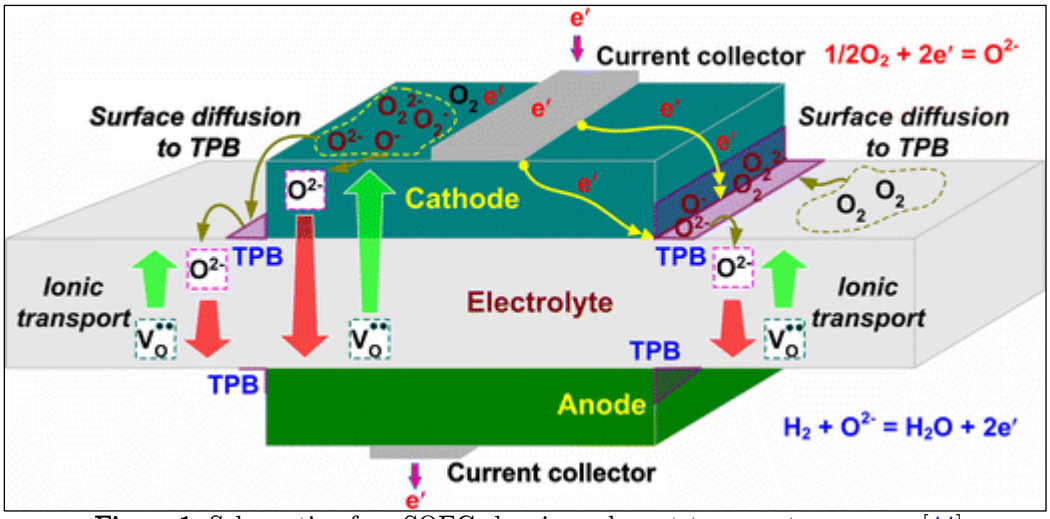

Figure 1. Schematic of an SOFC showing relevant transport processes [44]

2.2. SOFC Thermodynamics

In this section fundamental thermodynamic principles will be applied to derive the standard reversible voltage or the theoretical voltage that can be generated by an SOFC operating on Hydrogen.

From the first law we know that for a closed system the change in internal energy (dU) is equal to the heat transferred (dQ) to the system minus the work done (dW) by the system. Where the work done by the system is pressure-volume work when only mechanical work is considered

$$dU = dQ - dW \tag{2.4}$$

$$dU = dQ - pdV \tag{2.5}$$

The second law tells us that for a reversible heat transfer (dQ_{rev}) to a system at constant pressure and temperature (T) the entropy change (dS) of the system is given by

$$dS = \frac{dQ_{rev}}{T} \tag{2.6}$$

Combining equations (2.5)and (2.6) we get (2.7), which shows that the internal energy (U) of a system is a function of entropy (S) and volume (V)

$$dU = TdS - pdV \tag{2.7}$$

Using the first and second laws and equation (2.7) we obtain two other useful thermodynamic potentials which are functions of temperature, pressure and entropy. These are Gibbs free energy (G) and Enthalpy (H)

$$G = U - TS + pV \tag{2.8}$$

$$dG = -SdT + Vdp \tag{2.9}$$

$$H = U + pV \tag{2.10}$$

$$dH = TdS + Vdp \tag{2.11}$$

$$G = H - TS \tag{2.12}$$

The thermodynamic potentials shown above can be interpreted in simple terms as follows [43]. Internal energy (U) is the energy needed to create the system at constant temperature and pressure. Enthalpy (H) is the energy needed to create the system plus the work required to make space for it (negligible initial volume). Gibbs free energy (G) represents the energy required for creating a system at constant environmental temperature from a negligible initial volume minus the energy received from the environment.

It follows from the above definitions that Gibbs free energy is the net energy that is supplied by us to create the system therefore it must also be the maximum work that can be obtained from the system.

Differentiating equation (2.8) we get

$$dG = dU - TdS - SdT + pdV + Vdp \tag{2.13}$$

including electrical work in equation (2.5) we have

$$dU = TdS - (pdV + dW_{el}) \tag{2.14}$$

substituting dU from (2.14) in (2.13) gives

$$dG = -SdT + Vdp - dW_{el} \tag{2.15}$$

which for a constant temperature, constant pressure process gives

$$dG = -dW_{el} \tag{2.16}$$

Therefore the maximum electrical work that can be obtained from an SOFC can be determined by the Gibbs free energy change for the reaction involved (assuming a constant temperature, constant pressure process) as

$$W_{el} = -\Delta G_{rxn} \tag{2.17}$$

It should be noted that the constant temperature, constant pressure assumption signifies that the temperature and pressure should not change during the reaction and as long as that is true the above expression can be used to determine electrical work at any temperature and

pressure. This assumption is reasonable for a fuel cell operating at a constant temperature and pressure.

Electrical work potential is measured in terms of the developed voltage. Hence a relationship between Gibbs free energy change and voltage needs to be established. Now the electrical work associated with moving an amount of charge Q against an electric field with a potential V is given by

$$W_{el} = VQ \tag{2.18}$$

The amount of charge transferred is calculated as

$$Q = zF \tag{2.19}$$

where z is the number of moles of electrons released per mole of fuel during the reaction (z = 2 for Eq. (2.1)) and F is Faraday's constant.

From equations (2.28), (2.18)and (2.28) we get

$$V_{rev} = -\frac{\Delta G_{rxn}}{zF} \tag{2.20}$$

V_{rev} represents the reversible voltage or the theoretical maximum voltage that can be generated by a cell employing Hydrogen as the fuel. Assuming the reactants and products to be at standard state

$$V_{rev}^{o} = -\frac{\Delta G_{rxn}^{o}}{zF} \tag{2.21}$$

Equation (2.21) allows us to calculate the reversible voltage at standard state conditions (atmospheric pressure P_o, room temperature T_o and unit activities of all species) however the operating conditions of a typical SOFC can vary significantly from the standard state which has an influence on the calculated reversible voltage value. Figure 2 shows a thermodynamic model which can be used to determine the reversible work that can be obtained from a fuel cell operating on Hydrogen and Oxygen. The reactants and products must be compressed/expanded between their partial pressures (P_i) and the standard pressure. The net reversible work (W_{el}) obtainable from the fuel cell equals the sum of reversible works from the four conversion steps involved - compression/expansion of reactants (H_2,O_2), compression/expansion of the product (H_2O)and conversion of reactants to product at standard pressure.

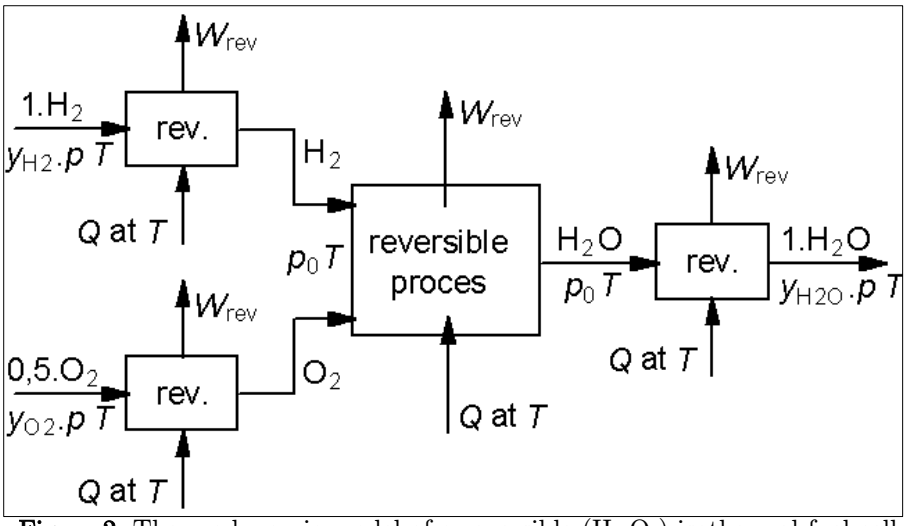

Figure 2. Thermodynamic model of a reversible (H_2-O_2) isothermal fuel cell

For an ideal gas, compression/expansion work is given by

$$W_{rev} = -nRT\int_{P_{in}}^{P_{out}}\frac{dp}{p} = nRT\ln\left(\frac{P_{in}}{P_{out}}\right) \tag{2.22}$$

$$W_{rev,H2} = RT\ln\left(\frac{P_{H2}}{P_o}\right) \tag{2.23}$$

$$W_{rev,O2} = 0.5RT\ln\left(\frac{P_{O2}}{P_o}\right) \tag{2.24}$$

$$W_{rev,H2O} = RT\ln\left(\frac{P_o}{P_{H2O}}\right) \tag{2.25}$$

For the conversion of reactants to products work is given by

$$W_{rev} = -\Delta G^o_{rxn} \tag{2.26}$$

Combining (2.23), (2.24), (2.25) and (2.26)

$$W_{el} = -\Delta G^o_{rxn} + RT\ln\left(\frac{P_{H2}P_{O2}^{0.5}}{P_{H2O}P_o^{0.5}}\right) \tag{2.27}$$

$$V_{nst} = V^o_{rev} + \frac{RT}{zF}\ln\left(\frac{P_{H2}P_{O2}^{0.5}}{P_{H2O}P_o^{0.5}}\right) \tag{2.28}$$

Equation (2.28) is known as the Nernst equation and V_{nst} is the Nernst voltage or the reversible voltage at any arbitrary temperature, pressure and species concentrations. It should be noted that the partial pressures of reactant and product species are bulk values.

In terms of mole fractions y_i and cell operating pressure P equation (2.28) can be written as

$$V_{nst} = V_{rev}^{o} + \frac{RT}{zF}\ln\left(\frac{y_{H2}y_{O2}^{0.5}}{y_{H2O}}\left(\frac{P}{P_o}\right)^{0.5}\right) \quad (2.29)$$

The voltage measured in a real SOFC deviates from the Nernst voltage due to a number of operational losses or irreversibilities which are described below.

Ohmic losses: are the losses which vary linearly with current and arise due to resistance to the flow of electrons through the electrodes, interfaces and current collectors and resistance to the flow of ions (oxide) through the electrolyte. These losses are dependent on electrical and ionic conductivities of the materials which in turn are temperature dependent.

Activation losses: represent the part of the available cell voltage sacrificed in order to overcome the activation barrier associated with the reaction (rate determining step) and produce a net current. Since these losses are related to the electrochemical reaction kinetics they tend to depend on a large number of factors such as operating temperature, pressure, concentrations of the reactants and products, type of catalyst and microstructure to name a few.

Concentration losses: these losses arise due to the resistance associated with the mass transport processes. Reactants must reach the triple phase boundary (TPB) or the reaction zone, while the products must be removed from the TPB. The main transport process involved is diffusion and therefore these losses depend on the concentrations and types of species diffusing, temperature and physical properties of the electrodes (porosity and tortuosity). Concentration losses affect the SOFC performance in two ways, first through the reversible voltage and second through activation losses since both are dependent on reactant and product concentrations at the reaction site.

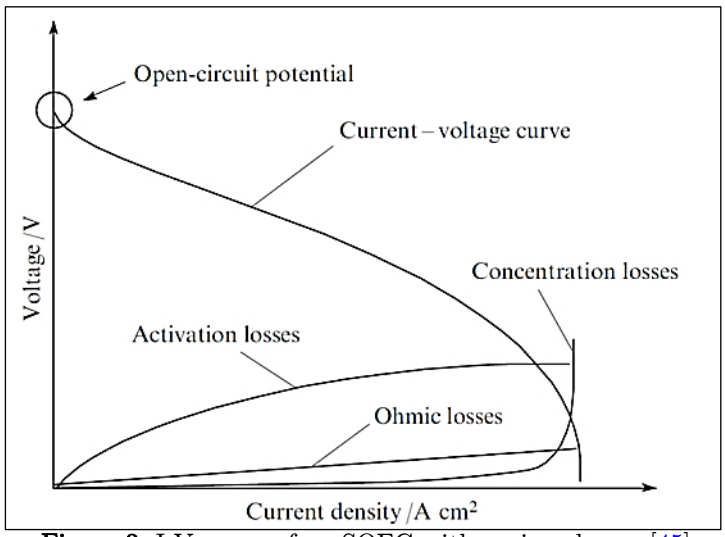

Figure 3. I-V curve of an SOFC with various losses [45]

Figure 3 shows an I-V curve of a typical SOFC along with the variation of the three losses discussed above with current density. As can be seen ohmic losses increase linearly with the current density, whereas activation and concentration losses show non-linear behaviour. Another observation that can be made is that activation losses dominate at lower current densities whereas concentration losses increase suddenly at high current densities. The reason for this phenomenon is that at very high current densities the rate at which the reactant species are consumed becomes higher than the rate of diffusion through the electrode which leads to a sudden drop in their concentrations at the reaction site and the cell becomes starved.

2.3. Exergy Analysis

Any thermodynamic system which is in disequilibrium with the environment has the potential to do work. The work would be maximized when the system is brought into equilibrium in an ideal way (through reversible processes). This maximum obtainable work is defined as the exergy of the system when only the environment is used as the reservoir of heat and matter. The system may be used to bring either an amount of energy or matter into equilibrium with the environment.

Exergy of matter is subdivided into two parts: Thermomechanical exergy (related to temperature and pressure differences w.r.t the environment) and Chemical exergy (related to chemical composition differences w.r.t the environment). Thermomechanical exergy represents the work obtained when the matter is brought to the environmental temperature and pressure while chemical exergy represents the amount of work obtained by isothermally converting the matter into environmental components at their respective partial pressures in the environment. Calculation of thermomechanical exergy requires the definition of environmental temperature and pressure and chemical exergy requires a reference environment composition.

The total exergy of a substance can be calculated as:

$$Ex_{total} = Ex_{thm} + Ex_{chem} \tag{2.30}$$

Thermomechanical exergy

It is defined as the maximum work that can be obtained when the matter is brought into thermomechanical equilibrium (temperature and pressure) with the environment.

$$Ex_{phy} = (H - H_o) - T_o(S - S_o) \tag{2.31}$$

Where enthalpy (H) and the entropy (S) of the system are calculated at its temperature and pressure (T, P) and the standard enthalpy (H_o) and entropy (S_o) for the same chemical composition are determined at the reference conditions of the environment (T_o, P_o).

Chemical Exergy

It is defined as the maximum work that can be obtained when matter is brought into chemical equilibrium (chemical composition) with the environment.

To evaluate a chemical exergy based on reference environment, there are two methods by Szargut (1967) and Baehr (1963). In the present work, Baehr environment is taken as the reference since it is used for evaluating energy conversion systems. In Baehr's method, mole or mass fractions of gaseous components in air at a reference temperature and pressure of 25°C and 1 atm respectively are provided as shown in Table 1.

Table 1. Baehr Reference Environment

Components	Mole Fractions
N_2	0.7565
O_2	0.2030
CO_2	0.0003
H_2O	0.0312
Ar	0.0090

The ideal processes used to determine the chemical exergy of a mixture are shown in Figure 4. It is assumed here that the components of the mixture have already been brought into thermomechanical equilibrium (P_o, T_o) and chemical equilibrium is achieved between steps 1 to 3a.

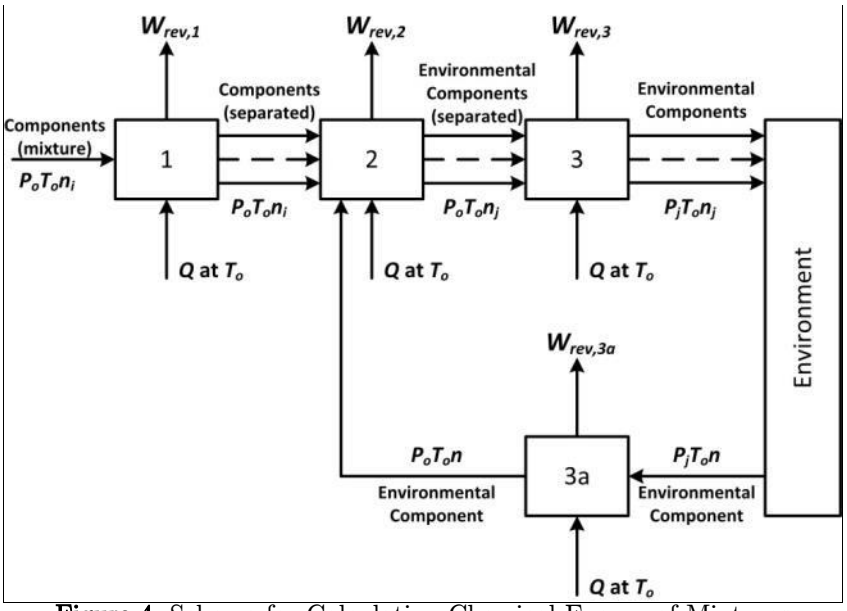

Figure 4. Scheme for Calculating Chemical Exergy of Mixtures

1. **Decomposition of the mixture:** Components of the mixture are separated and compressed and become available at (T_o, P_o). In case of a single compound, it is not required to separate the components therefore $W_{rev,1} = 0$. (For a mixture, equation 2.38 can be used)

2. **Chemical conversion into environmental components:** Separated components are converted into environmental components (e.g. CO_2, H_2O) by reacting with environmental components (e.g. O_2) (Reverse formation reaction)

$$W_{rev,2} = -[(H_{out} - H_{in}) - T_o(S_{out} - S_{in})] \quad (2.32)$$

3. **Expansion/compression of the environmental components:** Environmental components are expanded/compressed to their partial pressure, p_i in the environment

$$W_{rev,3} = -RT_o ln\left(\frac{p_i}{P_o}\right) \quad (2.33)$$

4. **Compression of environmental components for the reactions (usually O_2) (step 3a):** Compression of environmental component (transfer from environment through reversible membrane and compression) of separated component to environmental pressure.

$$W_{rev,3a} = RT_o ln\left(\frac{p_i}{P_o}\right) \quad (2.34)$$

The chemical exergy of the mixture is the sum of all the exergies calculated for the sub steps:

$$Ex_{chem} = W_{rev,2} + W_{rev,3} + W_{rev,4} + W_{rev,4a} \quad (2.35)$$

Calculation of chemical exergy of solid (eg. coal, wood) or liquid fuels for which the exact composition is not known is not trivial, but approximate determination can be carried out through empirical exergy factors f_{ex} published in literature, which relate it to the lower or higher heating values, where LHV and HHV represent the lower and higher heating values.

$$Ex_{chem,fuel} = f_{ex}(LHV_{fuel}) \quad (2.36)$$

Exergy efficiencies

Definition of exergy efficiencies is important for an exergy analysis of the system under consideration. Two types of exergy efficiencies are commonly used:

- Universal exergy efficiency
- Functional exergy efficiency

Universal exergy efficiency is simply defined as the ratio of exergy of the flows leaving the system to the exergy of flows entering the system.

Functional exergy efficiency is defined as the ratio of exergy of all the product flows to the exergy of all the source flows. Product exergy represents the total amount of useful work obtained from the system as product (such as work from a turbine or electric power from a fuel cell) and source exergy is the amount of exergy input to the system. Functional exergy

efficiency is the true efficiency and is preferred over universal exergy efficiency wherever a definition of products is possible.

Exergy losses

Exergy losses in 6 components - Compressors (or fans), Heat Exchangers, Fuel Cell, Combustor, Gas Turbine and Stack, are targeted in this study for optimizing the system efficiency. A brief description of the origins of losses in these components and strategies to minimize them are presented below-

Compressor losses mainly arise due to friction along the walls of the compressor. For a particular compressor and working fluid these losses increase with the pressure ratio and inlet temperature. When these parameters cannot be altered the only way to reduce the losses at the component level is to split the compression into a suitable number of stages and employ intercooling, thereby reducing the compression work [46]. At the system level these losses can be further reduced by minimizing the amount of excess air flow into the system or entirely avoiding the use of compressors/fans wherever possible (requires changes to system configuration).

Heat exchanger losses arise due to heat transfer at a finite temperature difference which is necessary to achieve heat transfer in a reasonable time with a small enough heat exchanger (larger equipment leads to higher pressure losses and costs). For air-air heat exchangers a temperature difference of 30 °C is considered reasonable, whereas for liquid-liquid heat exchangers it is taken as 15 °C. For a fixed value of temperature difference losses are higher if the absolute temperatures of the hot and cold streams are lower, therefore to reduce heat exchanger losses temperature differences should be minimized and heat exchange should be done at as high temperatures as possible.

Fuel cell losses have been explained in Chapter 2. At a system level fuel cell losses can only be reduced by trying to limit anode and cathode recirculation thereby limiting dilution of the fuel and air or by distributing the total fuel utilization over two (or more) fuel cells stacks connected in series [33] and employing intercooling between the stacks (depending on the temperature dependence of the cell resistance).

Combustor losses are the result of the irreversible combustion process and the proceeding heat transfer losses (from the flue gas to the working fluid). Although with an efficient combustor and heat exchanger design energy efficiencies of about 90% (and higher) can be achieved but exergy losses still remain significant due to the fact that the chemical exergy of the fuel is higher than the LHV (which varies with the type of fuel). In commercially available Gas turbines the combustor is located just before the turbine inlet and within the same enclosure therefore the heat transfer is instant (as flue gas is the working fluid) which leads to even higher energy efficiencies. System efficiencies can be improved further if the

combustion temperature is increased by use of preheating and reducing the air factor (defined as the ratio of actual air flow in the combustor to the stoichiometric air flow required) but in most gas turbines material limitations force the turbine inlet temperature to be significantly lower than the adiabatic temperatures that can be achieved (even when using air as the oxidizer). The only way to reduce combustor losses beyond a point is to use fuel cells which can achieve an almost reversible conversion of the chemical exergy of the fuel to electric power.

Gas turbine losses also arise mainly due to friction (as is the case for compressors). During adiabatic expansion a part of the heat produced due to friction can be converted into work and this proportion increases with an increase in the temperature at which this heat is produced. Therefore gas turbine losses can be reduced by increasing the turbine inlet temperature as much as possible (within the material limitations). Increasing pressure ratio also leads to a slight improvement in the efficiency but this is limited by the consequent increase in compression losses so for a particular turbine an optimum pressure ratio needs to be determined for each system (since pressure losses within the system dictate the difference between the compressor and turbine pressure ratio).

Stack (chimney) loss simply represents the heat transferred to the environment along with the flue gas. The higher the temperature of the flue gas leaving the system, the higher will be the loss. At the component level nothing can be done to reduce this loss but at the system level better heat management will lead to a lower stack temperature. Utilization of residual heat elsewhere (for district heating or as low temperature process heat) is another option for reducing stack loss (by converting it into a useful product) and improving overall system efficiency.

2.4. Carbon Deposition

When using carbonaceous fuels (such as Methane, Methanol, Natural Gas or Biosyngas etc.) along with SOFCs, carbon deposition can be an issue in the anode inlet pipe or the anode surface. Under load when current is being extracted from the cell (especially at higher current densities) the oxygen partial pressure at the anode is high therefore there is a lower tendency of carbon deposition on the anode surface as compared to the inlet pipe. Traditionally steam/methane or steam/carbon ratios have been studied in order to determine safe operating conditions with respect to carbon deposition in SOFC system studies. The reported values of steam to carbon ratio vary from 0.5 to 3 (and above) [47, 48] and there seems to be no consensus on a particular value. Additionally when the fuel stream consists of carbonaceous fuels along with CO, CO_2 or H_2 these ratios become misleading since CO and CO_2 have a different impact on the carbon deposition tendency. As a result some values of steam/carbon ratios end up being under-safe while some are over-safe. Therefore the correct and more effective way of determining carbon deposition tendencies at varying

operating conditions (fuel composition, temperature and pressure) is to use the C-H-O ternary plots.

Figure 5 presents a C-H-O ternary plot with carbon deposition boundary lines at different temperatures and pressures. Each point on the solid boundary line inside the triangle represents a different C-H-O ratio and thus a different composition. The plot is generated using Factsage, a thermochemical software for performing equilibrium calculations [49]. The software is also used in this study to determine carbon deposition free operating conditions in system modeling with Methane. From the composition of the fuel stream its coordinates on the plot are determined and if those coordinates lie above the corresponding boundary line then carbon deposition is favoured thermodynamically while if they lie below the line there is no deposition.

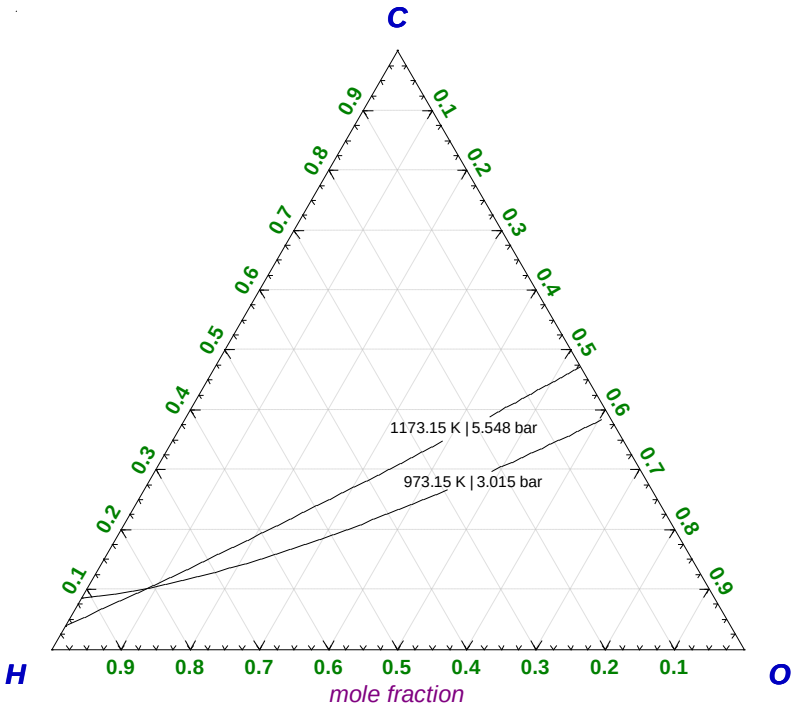

Figure 5. Ternary Phase Diagram Indicating Carbon Deposition Regions

2.5. Cycle Tempo – Calculation Rules

Cycle Tempo is a software developed in-house at TU Delft for designing, analyzing and optimizing the thermodynamics of energy conversion systems. It uses a Gibbs free energy minimization routine for determining equilibrium compositions in the fuel cell and the combustor models used in this study. More details about these models can be found in the Cycle Tempo manual [50].

In this work, a choice is made to fix the gas turbine power at 30 kW which determines the mass flow rates through the system. Power output and therefore the area of the fuel cell vary

with the fuel flow. An energy balance for the fuel cell determines the cathode airflow based on the cooling demand. Some basic equations governing the processes in the fuel cell and the gas turbine as used in the Cycle-Tempo calculations are given below. In order to calculate the current density, cell voltage and electrical power a one dimensional model of the fuel cell is considered. Temperature and pressure are assumed to be constant in the direction perpendicular to fuel flow. Local variables at a cross section x along the length of the fuel cell are calculated as follows.

$$I = \frac{\varphi_{m,a,in}}{M_a} 2F\left(y_{H_2} + y_{CO} + y_{CH_4}\right)U_f \tag{2.37}$$

where I is the current, $\varphi_{m,a,in}$ is the mole flow rate at the anode inlet, y_i are the mole fractions at the cell inlet, M_a is the molar mass of the fuel stream at the anode inlet, F is Faraday's constant and U_f is the fuel utilization. The mass flow of Oxygen from cathode to anode is calculated using the current flow.

$$V_{rev,x} = V_{rev}^{o} + \frac{RT}{2F} \ln\left(\frac{y_{H_2} y_{O_2}^{0.5}}{y_{H_2O}} \times P_{cell}^{0.5}\right) \tag{2.38}$$

where V_{rev}^{o} is the standard reversible voltage (standard Nernst potential) for Hydrogen, R is the universal gas constant, T the cell temperature, y_i the mole fraction of species i at cross-section x and P_{cell} is the ratio of cell operating pressure to standard pressure P_o. Voltage losses in the $x-$ direction (along the length of the cell) are assumed to be negligible as a result the operating cell voltage is constant over the fuel cell. Voltage loss at cross section x is given by

$$\Delta V_x = V_{rev,x} - V \tag{2.39}$$

With R_{eq} being the equivalent cell resistance, current density at cross section x is calculated as

$$i_x = \frac{\Delta V_x}{R_{eq}} \tag{2.40}$$

Over the complete cell area we have

$$\frac{I}{A} = \frac{U_f}{R_{eq} \int_0^{U_f} d\lambda/(V_{rev} - V)} \tag{2.41}$$

where I is the total current, A the cell area and λ the reaction coordinate (dimensionless). For design calculations, current density, operating voltage and fuel utilization are specified and cell resistance and area are calculated. For a achieving a specific resistance value the

specified operating voltage needs to be adjusted each time. It should also be noted that the cell operating voltage is mainly decided by the reversible voltage at the outlet of the cell as it cannot be higher than the lowest potential on the anode (which is at the cell outlet).

For the turbine outlet enthalpy is calculated as

$$h_o = h_i - \eta_s(h_i - h_{o,s}) \tag{2.42}$$

Where h_o is the specific enthalpy at the outlet, h_i the specific enthalpy at the inlet, $h_{o,s}$ the specific enthalpy at the outlet for isentropic expansion and η_s the isentropic efficiency. For the compressor we have

$$h_o = h_i + \frac{(h_{o,s} - h_i)}{\eta_s} \tag{2.43}$$

Universal exergy efficiency can be calculated as

$$\eta_{ex,el} = \frac{\sum Ex_{products}}{\sum Ex_{source}} \tag{2.44}$$

where products and source refer to outgoing and incoming exergy flows in the system respectively. Proper definition of products and source is required in order to calculate functional exergy efficiencies. System electrical exergy efficiency is calculated as

$$\eta_{ex,el} = \frac{\sum P_{el,out} - \sum P_{el,in}}{Ex_{fuel,in}} \tag{2.45}$$

where $P_{el,out}$ and $P_{el,in}$ are output and input electrical power of the system. Total system exergy efficiency is given by

$$\eta_{ex,tot} = \frac{\sum P_{el,out} + \sum Ex_{heat,out} - \sum P_{el,in}}{Ex_{fuel,in}} \tag{2.46}$$

Further details regarding the software and the calculation procedure can be found here [50].

3

System Modeling

3.1. Model Description

The base model considered here consists of an SOFC connected with a Gas Turbine (GT) which utilizes the exhaust of the SOFC. Fuel is sent to a compressor along with the required amount of water. The heat of evaporation for the water is provided in the following fuel preheater which utilizes the exhaust of the gas turbine. A fraction of the SOFC exhaust (both anode and cathode) is recirculated for maintaining cell inlet temperatures. The unutilized fuel left at the fuel cell outlet is sent to the combustor along with the air from the cathode outlet. The flue gas produced is then supplied to the GT. The GT exhaust is used for preheating fresh air and fuel streams. In consequence the whole system becomes comparable to a recuperated GT.

The GT power is fixed at 30 kW while the fuel cell output is allowed to vary, as a result of which the fuel cell size is different for different operating conditions. Fuel cell inlet and outlet temperatures are specified and these in turn determine the recycle ratios. The cell operating temperature is taken as the average value of the inlet and outlet temperatures and is used for equilibrium calculations within the cell. Fresh fuel is 100% Hydrogen for the case with Hydrogen and 80% Methane with 20% water for the case with Methane. Table 2 and Table 3 present the model input parameters and the fuel cell resistance at different temperatures respectively. The model is presented in Figure 6 below.

Table 2. Model Input Parameters

Parameter	Value
Isentropic efficiency of turbine and compressor (502)	78%
Mechanical efficiency of turbine and compressor	98%
Isentropic efficiency of compressors (102,109,206)	75%
Mechanical efficiency of compressors (102,109,206)	95%
Fuel Cell Operating Temperature	850 ^{0}C
Fuel Cell Inlet Temperature	800 ^{0}C
Fuel Cell Outlet Temperature	950 ^{0}C
Fuel Cell Resistance	6.563 x 10^{-5} Ωm^2
Overall Fuel Utilization	85%
Current Density	2500 A/m^2
Operating Voltage	0.7467 V
Fuel Cell Pressure	2.975 bar
Air, Fuel Inlet Pressure	1.01325 bar
Pressure Ratio	3

Table 3. Fuel Cell Resistance [51]

Temperature [^{0}C]	Resistance [Ω-cm^2]
750	1.3750
800	0.9063
850	0.6563
900	0.4900
950	0.2724*

* extrapolated

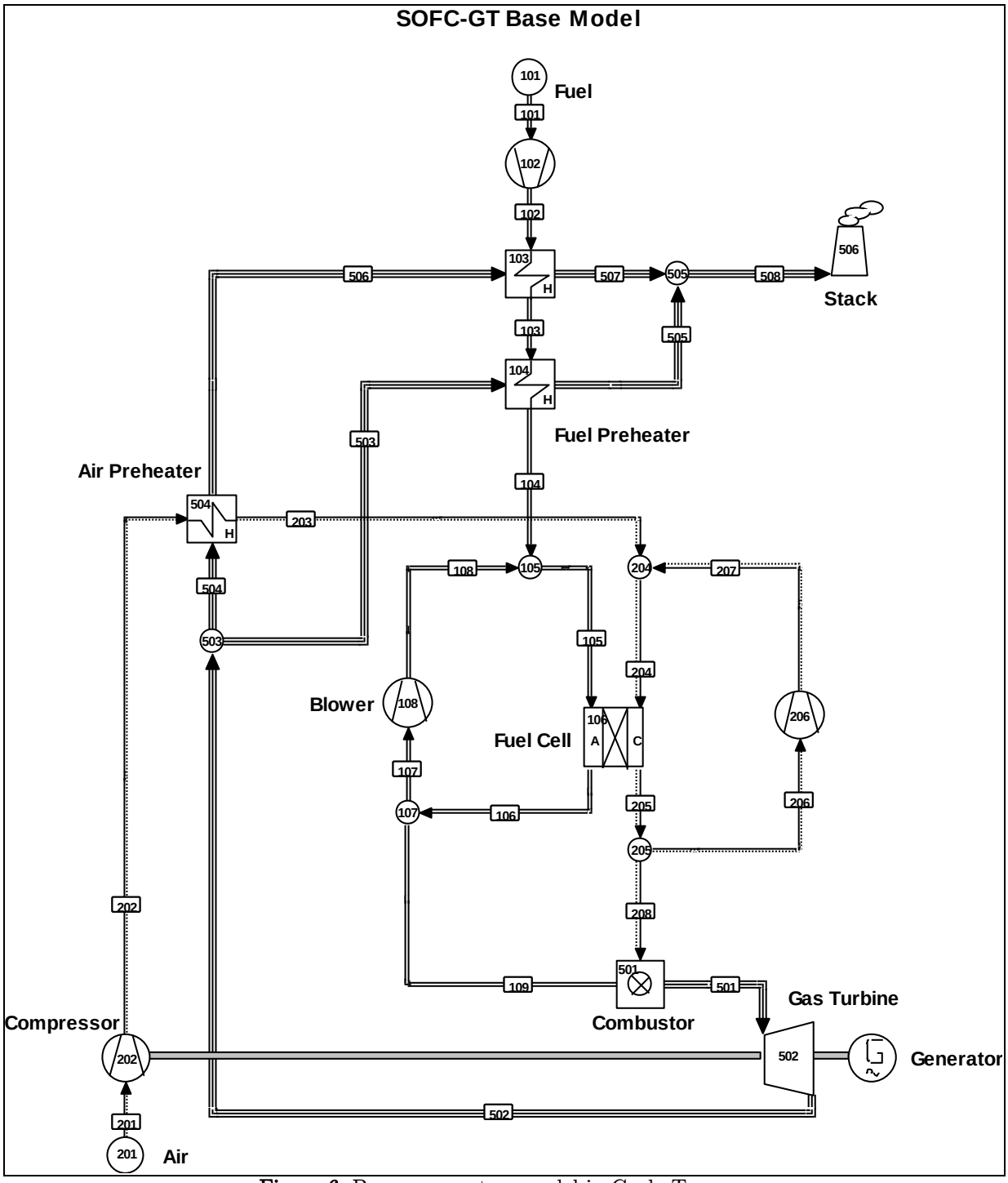

Figure 6. Base case system model in Cycle Tempo

Table 4 presents the results for the base case model with Hydrogen and Methane as fuels. The different losses and their respective causes will be discussed later. With Hydrogen the fuel cell produces 73.4 kW (cell area 39.34 m^2). Per pass fuel utilization of 71.83% is achieved with fuel and air recirculation ratio being 9.47 and 0.68 respectively. System efficiency of 69.91% (energy efficiency 68.49%) is achieved. On the other hand with Methane as the fuel, the fuel cell produces 144.9 kW (cell area 73.92 m^2). Per pass fuel utilization is 80.8% (fuel recirculation ratio 1.26). System efficiency of about 74% (energy efficiency 76.74%) is achieved.

Table 4. Base Case Results

Parameter	Hydrogen	Methane
Exergy Efficiency	69.91%	73.99%
Energy Efficiency	68.49%	76.74%
Fuel Recycle Ratio	9.47	1.26
Air Recycle Ratio	0.68	0.12
Air Factor	33.76	15.93
Fuel Cell Power	73.4 kW	144.9 kW
Per Pass Fuel Utilization	71.83%	80.80%
Per Pass Air Utilization	8.95%	24.02%

Exergy losses in different system components are shown in the exergy flow diagrams in Figure 7 and Figure 8. These figures depict exergy losses and power produced as percentages of the input exergy of the fuel. As can be seen, with Hydrogen the compressor, gas turbine (expander) and stack losses are higher in comparison to Methane while fuel cell losses are lower. Higher losses in these components follow from higher air flows (relative to the system size) or more precisely higher air factor with Hydrogen. The higher air factor also implies a higher proportion of power produced in the GT thereby leading to lower system efficiency with Hydrogen. As discussed in [40] fuel cell losses are higher with Methane due to the higher per pass fuel utilization which leads to a higher drop in the Nernst voltage between the inlet and the outlet of the cell.

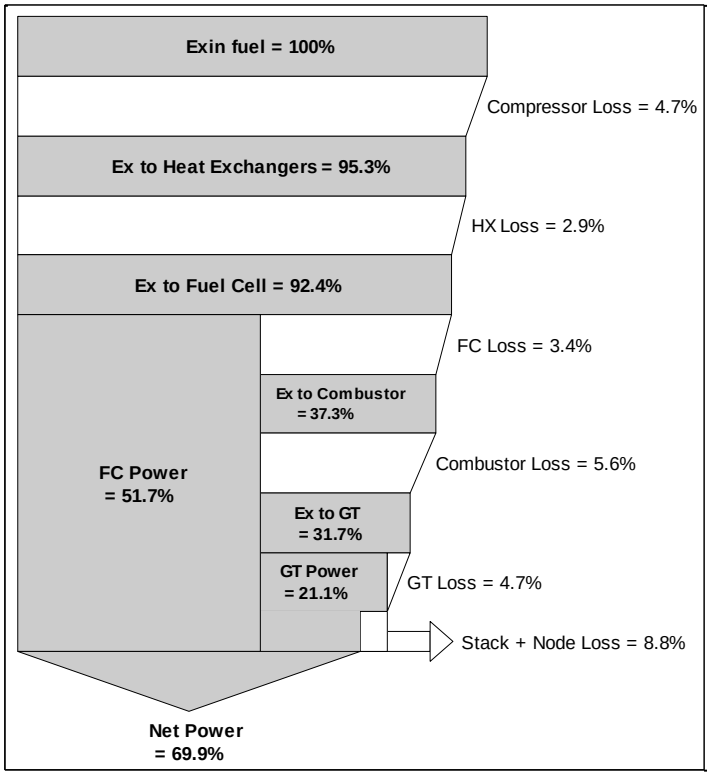

Figure 7. Exergy flow diagram – Base Case Hydrogen

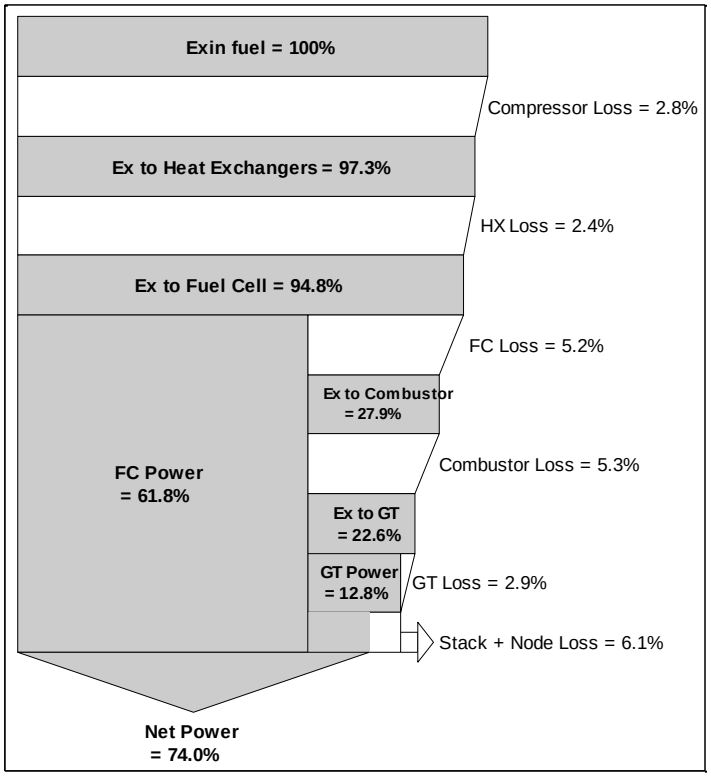

Figure 8. Exergy flow diagram – Base Case Methane

3.2. Sensitivity Analysis - Hydrogen

Temperature Variation

To study the effect of variation of temperature on system efficiency the cell temperature is varied from 750-950°C. Increasing cell temperature is accompanied by a decrease in the Standard Nernst potential which implies an increase in the fuel cell losses. In the considered temperature range the Standard Nernst potential decreases by about 5.9%. This translates to a 7.1% and 8.5% decrease in the reversible voltage at the cell inlet and outlet respectively. However with increasing temperature the cell resistance drops strongly (80.2%) leading to an increase of 31.9% in the operating cell voltage. The combined effect of these two phenomena is an increase in fuel cell efficiency with temperature and a decrease in fuel cell losses.

An increase in cell outlet temperature leads to an increase in the turbine inlet temperature. This leads to an increase in the specific work output (and to a certain extent the efficiency) of the gas turbine. As a result, the air flow rate required by the turbine to produce the specified power decreases. In addition, due to the increase in the cell efficiency the specific heat production (w.r.t fuel flow rate) in the cell goes down which further reduces the amount of air flow in the system. This reduction in the air flow rate due to these two causes makes the increase in turbine inlet temperature (226 K) greater than the increase in cell outlet temperature (200 K). A reduction in the air flow rate also leads to reduction in the air compressor and stack losses (stack temperature practically remains constant). Combustor losses decrease as well due to the lower air factor. Figure 9 presents the variations in relative and absolute exergy losses with cell temperature.

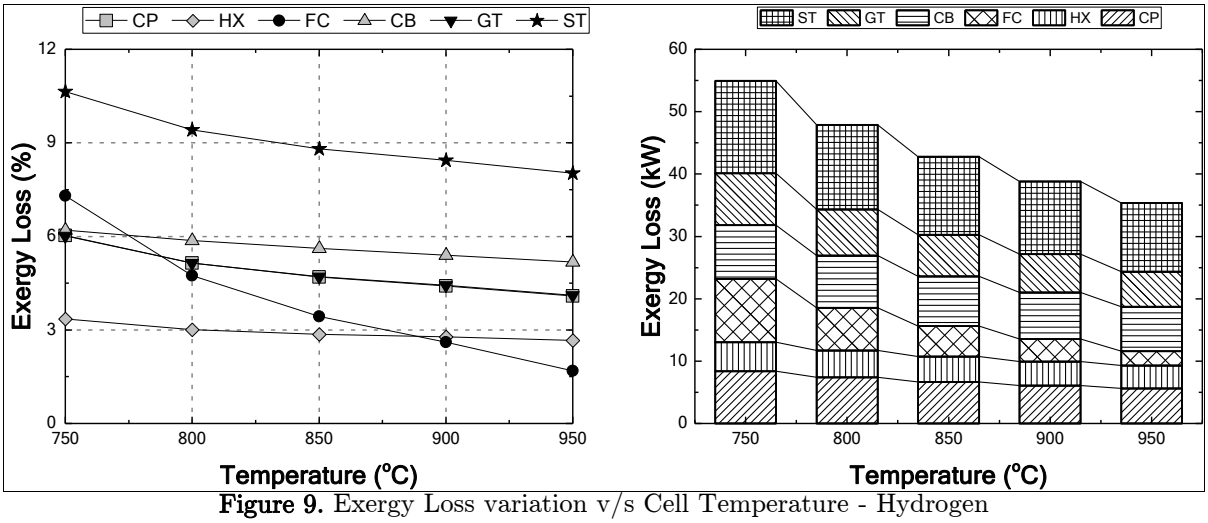

Figure 9. Exergy Loss variation v/s Cell Temperature - Hydrogen

On the other hand a reduction in the specific heat production (w.r.t fuel flow rate) in the cell implies that a lower amount of heat is available for the gas turbine for a particular fuel flow rate. In order to compensate for this effect the fuel flow rate in the system increases very

slightly (between 750-800°C) and the turbine is able to produce the specified power. From 800°C onwards the increase in specific output (w.r.t air mass flow rate) of the turbine compensates for the reduction in specific heat production in the cell and the fuel flow rate decreases steadily. This is due to the fact that from 750-800°C there is a sudden decrease in cell resistance (so specific heat production) whereas from 800-950°C the change is gradual.

An increase in the turbine inlet temperature is followed by an increase in the turbine outlet temperature as the pressure ratio is fixed. Since the turbine exhaust is used for preheating, the temperatures of the fresh air and fuel streams also increase by 21.6% and 18.1% respectively. On the other hand, the increase in cell inlet and outlet temperature is about 20.6% and 18.6% respectively, therefore in order to maintain the cell temperature the fuel and air recirculation ratios increase. Air recirculation ratio increases by 7.2% whereas fuel recirculation ratio increases by 29.3% as the increase in fresh fuel temperature is lower than the increase in the cell inlet temperature. Figure 10 depicts the trends in system efficiency and other variables with cell temperature. Net specific output is defined as the ratio of net electrical power (from the GT and the fuel cell) to the air flow rate.

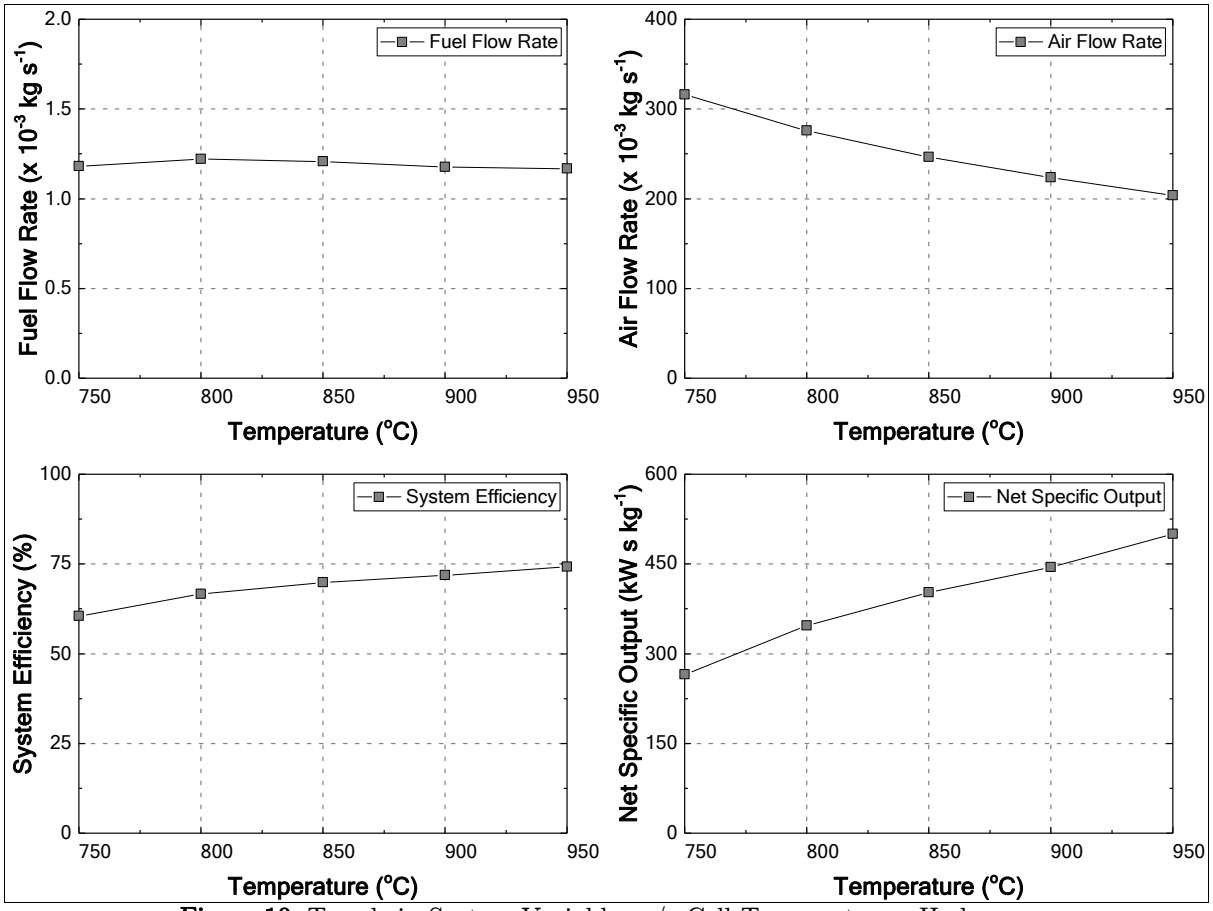

Figure 10. Trends in System Variables v/s Cell Temperature - Hydrogen

As overall fuel utilization rate and GT power are fixed an increase in the fuel cell efficiency also leads to an increase (~5.7%) in the proportion of power produced by the fuel cell. This is confirmed by the fact that the flow rate of fresh fuel in the system decreases from 800°C and the fuel flow rate to the combustor also decreases by the same amount. The additional power output from the fuel cell is therefore solely due to the increase in efficiency (as indicated by a 31.9% increase in the cell operating voltage). Increasing turbine inlet temperature leads to a slight increase in GT efficiency as well. The overall increase in the system efficiency is about 13.8% and this is largely due to the higher efficiency of energy conversion in the SOFC.

Pressure Ratio Variation

In order to study the impact of pressurization on system efficiency the pressure ratio was varied from 2-5.5 at a cell operating temperature of 950°C while the remaining parameters in Table1 were kept constant. Since the fuel cell operating temperature is fixed, the maximum turbine inlet temperature remains more or less fixed (increases slightly, explained below) therefore with an increasing pressure ratio the turbine outlet temperature drops (12.1%).

At higher pressure ratios the temperatures of the fresh air and fuel streams just after compression increase, however due to the lower turbine outlet temperatures the temperatures of both the streams after preheating decrease by 12.4% and 12.5% respectively. As a result the fuel and air recirculation ratios increase (109% and 852% respectively) to maintain the fuel cell inlet temperature. Increasing fuel recirculation in turn reduces the per pass fuel utilization. This reduction in per pass fuel utilization implies an increasing dilution of the fuel at the inlet but an improvement in the reversible voltage due to increasing pressure still leads to an increase in the cell efficiency. As explained in the temperature variation section, an increase in the cell efficiency leads to a reduction (64.8%) in the air factor in the combustor and consequently a slight increase (5.1%) in the turbine inlet temperature. Air flow rate mainly reduces due to increasing specific output of turbine at higher pressure ratios. Gas turbine losses increase due to higher specific entropy production but the increase is mitigated slightly by the reducing air flow rate and increasing turbine inlet temperature. Compressor losses decrease slightly till a pressure ratio of 3 and then increase (due to a strong decrease in the air flow rate till pressure ratio 3). Net specific output of the gas turbine increases with increasing pressure ratio, however this is achieved at the cost of gas turbine efficiency (turbine and compressor) as confirmed with increasing specific losses in both the turbine and compressor. This increase in losses leads to an increase in the fuel flow rate at pressure ratios above 3. Figure 11 shows the variation in fuel and air flow rate with pressure ratio.

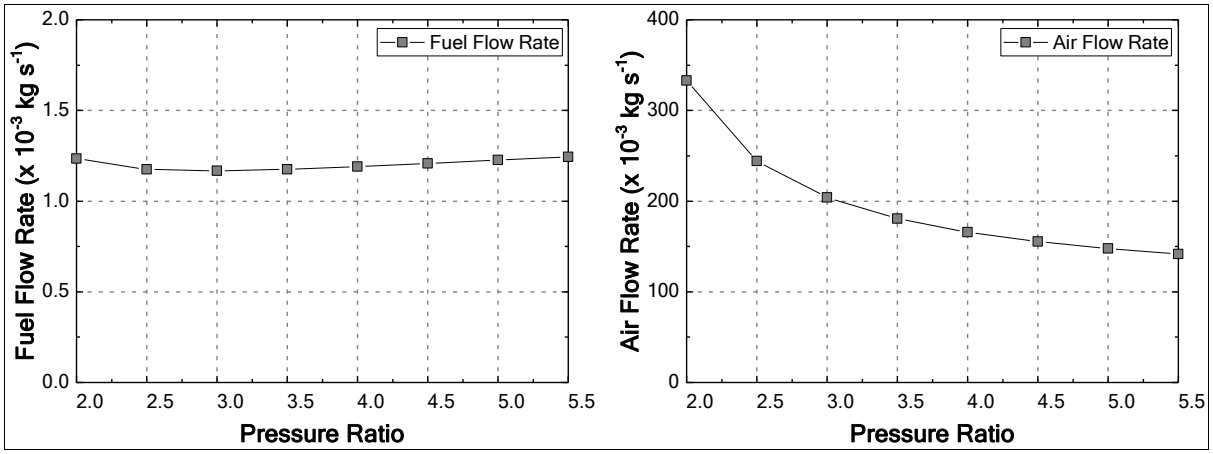

Figure 11. Fuel Flow, Air Flow v/s Pressure Ratio – Hydrogen

A reduction in the fresh air flow rate also leads to a reduction in the heat exchanger losses (transmitted heat flow decreases). A decreasing air flow combined with a slight increase in the turbine inlet temperature should lead to a steady decrease in combustor losses. However due to an increasing fuel flow rate combustor losses start to increase slightly after a pressure ratio of 4.5. Despite a reduction (57.4%) in the air flow rate stack losses increase as the stack temperature goes up by 37.3% (to 274.8°C). This is due to an increase in the compressed air and fuel temperatures before preheating and to a slight extent an increase in the steam content in the flue gas.

Interestingly the reversible voltage increases (2.8%) at the outlet of the cell and decreases (8.7%) at the inlet while the operating voltage increases by about 0.9%. This happens as the composition at the outlet of the cell remains fixed due to the constant overall fuel utilization and the reversible voltage simply increases with the increasing pressure ratio. On the other hand, at the inlet of the cell the concentration of Hydrogen decreases (and that of water increases) due to the increasing recirculation rate, nullifying the positive effect of the increasing pressure ratio on the reversible voltage therefore fuel cell losses decrease only slightly. Figure 12 shows the variation in exergy losses with pressure ratio.

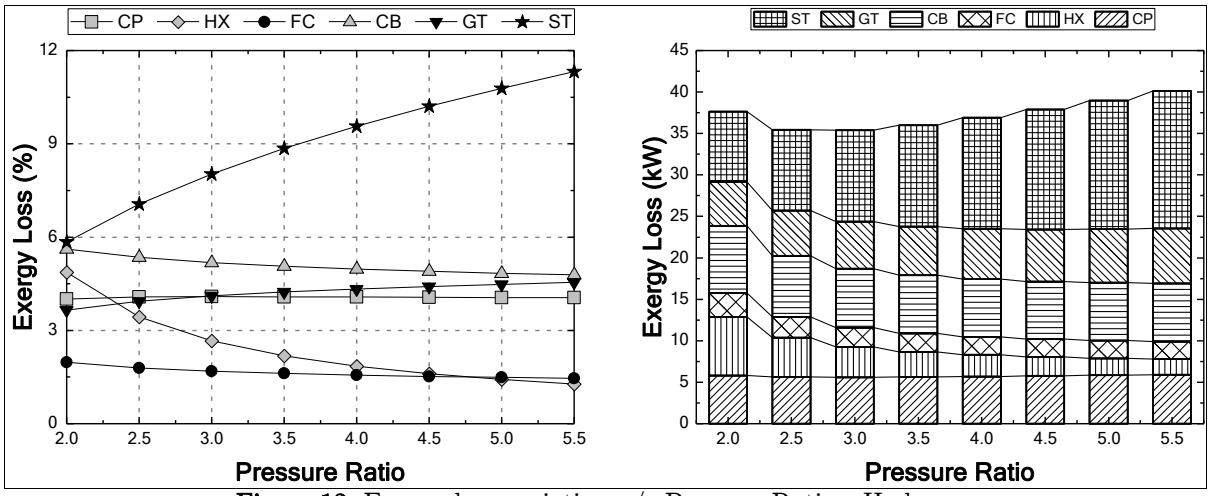

Figure 12. Exergy loss variation v/s Pressure Ratio - Hydrogen

Figure 13 below shows the variation of system efficiency, specific output (w.r.t air mass flow) and specific fuel consumption with increasing pressure ratio. System efficiency increases, attains an optimum at a pressure ratio of 2.5 and then decreases. As the pressure ratio increases (2-5.5) the temperature of the compressed air (and fuel) stream increases, as a result the amount of fuel required to achieve the turbine inlet temperature (which remains fixed as explained above) decreases which leads to an increase in cycle efficiency. The use of turbine exhaust for preheating the fuel and air flows at the combustor inlet leads to a further increase in the efficiency and a reduction in the optimum pressure ratio. It should be noted that the optimum pressure ratio is a function of the turbine inlet temperature and increases with it. Above the optimum pressure ratio, the increase in compression work outweighs the positive effect of reduction in the fuel flow (compressor outlet starts approaching the turbine outlet temperature, reducing the amount of heat that can be recovered) and the system efficiency decreases. This behaviour is characteristic of practical regenerative gas turbine cycles [46]. Specific output increases at a decreasing rate with pressure ratio in the considered range. At even higher pressure ratios the specific output would achieve a maximum value and then decrease. This maximum value depends on the turbine inlet temperature, pressure ratio and the nature of the working fluid (adiabatic ratio γ). The decrease in specific output at higher pressure ratios is due to the fact that compression work starts to approach the turbine work. Specific fuel consumption initially decreases with pressure ratio, attains a minimum value and then increases again.

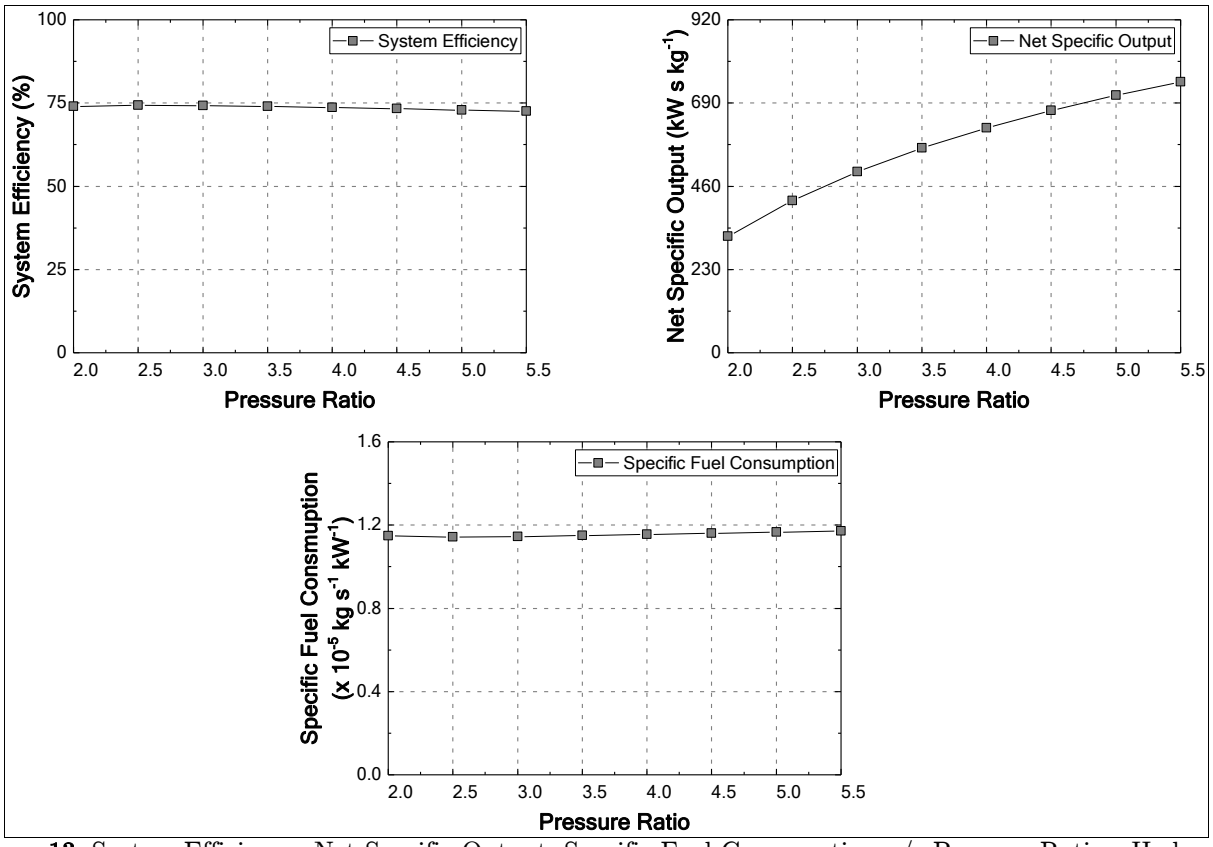

Figure 13. System Efficiency, Net Specific Output, Specific Fuel Consumption v/s Pressure Ratio - Hydrogen

Fuel Utilization Variation

Keeping all model input parameters from Table 1 constant the overall fuel utilization is varied between 75-95%. As fuel utilization increases the fuel cell efficiency goes down and the specific heat production in the cell increases, which further leads to an increase in the air flow rate in order to satisfy the increased cooling load. This leads to a decrease in the turbine inlet temperature (7.2%) and therefore the specific output of the turbine. As a result the air flow rate increases by 17.1% (since a lower air flow is required by the turbine to produce the specified power). Since a higher proportion of fuel is being utilized in the fuel cell the fresh fuel flow rate in the system increases (26.6%) as expected in order for the turbine to produce the specified power. Despite the increase in the air flow rate being lower than the increase in fuel flow rate, the air factor in the combustor increases significantly. This is due to a decrease in the moles of Hydrogen in the fuel stream (LHV decreases by 80%) entering the combustor which is expected with higher fuel utilization in the cell. This also leads to a reduction in the combustor losses since a lower amount of fuel is combusted. Increasing air flow leads to an increase in the compressor, heat exchanger and turbine losses as well, as seen in Figure 14 with absolute losses. In relative terms these losses decrease since the increase in fuel cell and stack losses is much higher.

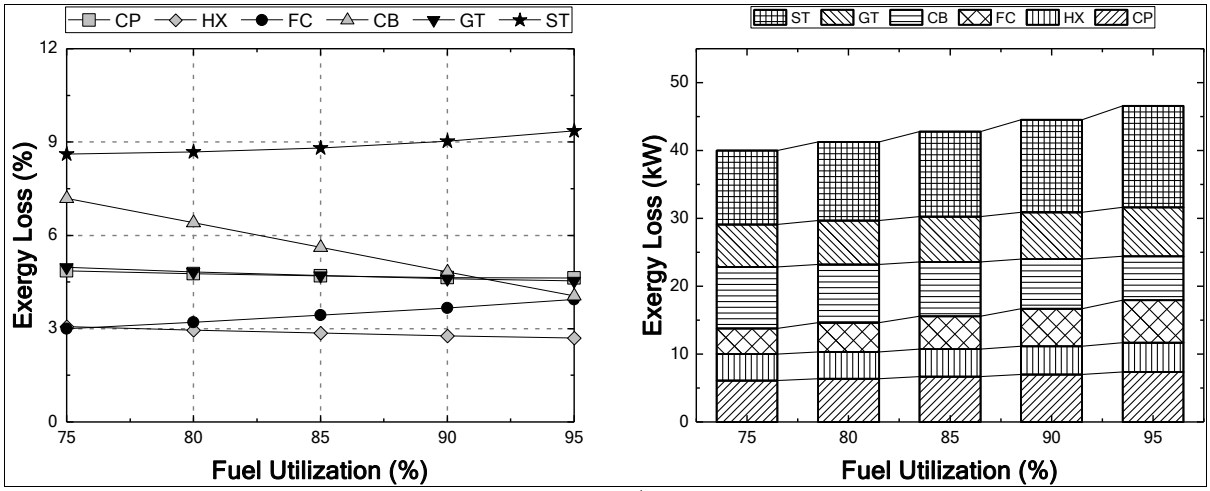

Figure 14. Exergy Loss variation v/s Fuel Utilization - Hydrogen

Following the decrease in the turbine inlet temperature the turbine outlet temperature decreases (7.4%) as well. As seen in the temperature variation section, the turbine outlet temperature directly affects the temperatures of the fresh fuel and air streams (due to its use for preheating) which also decrease. Since the fuel cell inlet and outlet temperatures are fixed, a reduction in the fresh air temperature leads to an increase in the air recirculation rate (186%). Fuel recirculation also increases (272%) in order to maintain the cell inlet temperature. Although the fresh air and fuel temperatures reduce by the same amount (7.6%), the increase in fuel recirculation ratio is significantly higher in comparison to air recirculation due to the increasing difference between the specific heat capacities of the fresh fuel (100 % Hydrogen) and the anode exhaust (25 – 5 % Hydrogen).

As expected, increasing fuel utilization in the cell leads to an increase in the proportion of power produced by it and hence higher system efficiency (3.5%) even though the fuel cell efficiency itself decreases with increasing utilization. A reduction in the turbine inlet temperature combined with an increasing air flow rate leads to an increase in turbine losses as well. Calise et al [36] also reported a similar conclusion with increasing fuel utilization for a natural gas fed SOFC-GT system. Figure 15 presents the trends in system efficiency and other variables with fuel utilization.

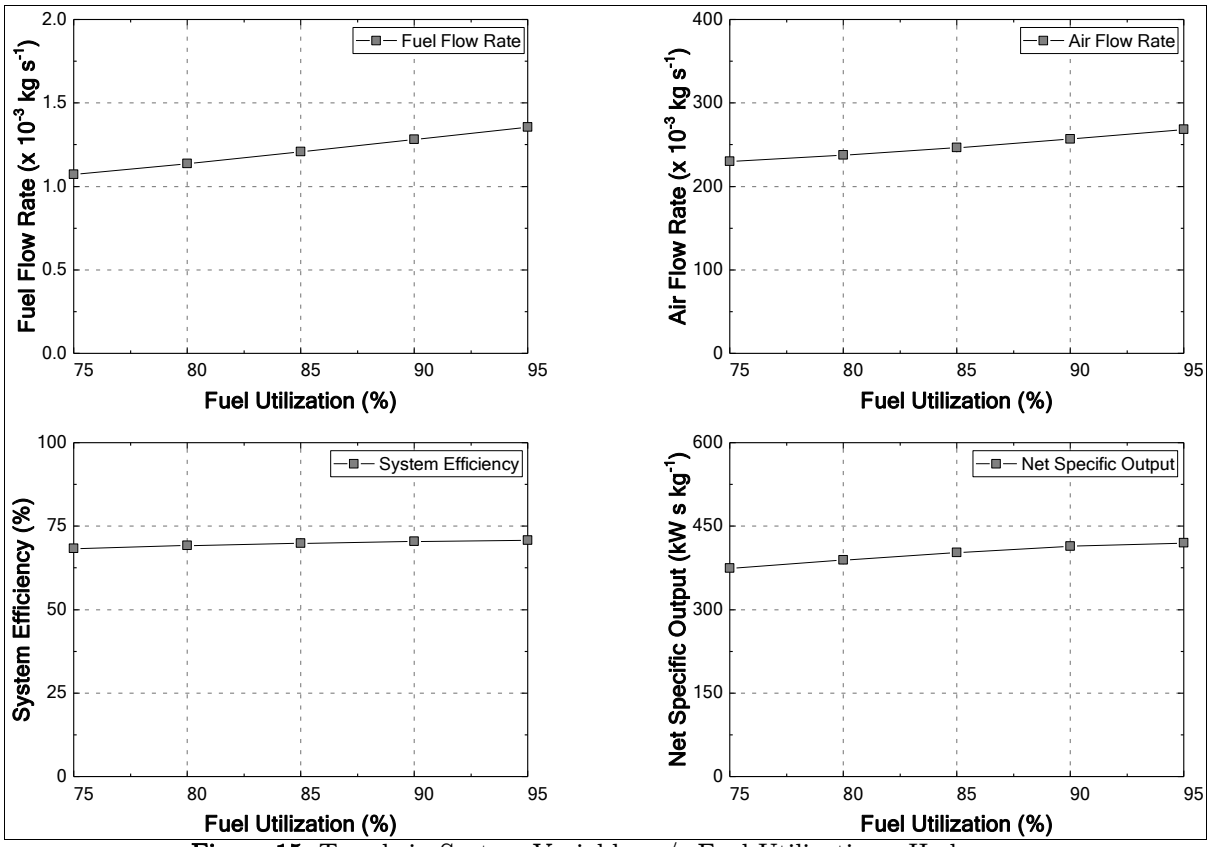

Figure 15. Trends in System Variables v/s Fuel Utilization - Hydrogen

3.3. Sensitivity Analysis - Methane

Temperature Variation

As with the Hydrogen base model above, the variation of cell temperature from 750 - 950^{0}C is accompanied by a decrease (same as before) in standard Nernst potential which leads to a decrease in the reversible voltage at the inlet and outlet of the cell. The cell operating voltage increases by 10.9% due to a strong decrease in the cell resistance and the cell efficiency increases overall. As explained in the Hydrogen section this increase in cell efficiency combined with an increase in specific output of the turbine leads to a reduction in the fresh air flow rate (39%) which lowers the air factor in the combustor and leads to an

increase in the turbine inlet and outlet temperatures. As a result the temperatures of the fresh fuel and air streams after preheating increase by 28.96% and 24.8% respectively. With the increase in cell inlet temperature from 700-900°C (20.6%) being lower than both, the fuel and air recirculation ratios decrease by 47.3% and 85.2% respectively. The reduction in the air recirculation rate is much higher since the fresh air temperature after preheating is closer to the cell inlet temperature (in comparison with the fresh fuel temperature) and due to a much higher reduction in the fresh air flow rate which reduces the amount of heat required to achieve the cell inlet temperature.

Fuel flow rate increases initially until a temperature of 850^{0}C and then decreases slightly with the overall result being an increase of 11%. As explained in the Hydrogen section this is a result of a stronger decrease in specific heat production in the cell compared to the increase in specific output of the turbine between 750-850°C. At higher temperatures the increase in specific output of the gas turbine is sufficient to overcome the reduction in specific heat production in the cell therefore the fuel flow decreases slightly. An increase in fuel cell efficiency combined with the increasing fuel flow rate leads to an increase (~5.4 %) in the proportion of power produced by the fuel cell. As expected turbine efficiency increases slightly with an increasing turbine inlet temperature and the system efficiency increases by about 13.5%. Figure 16 shoes the trends in system variables with cell temperature while Figure 17 presents the exergy losses.

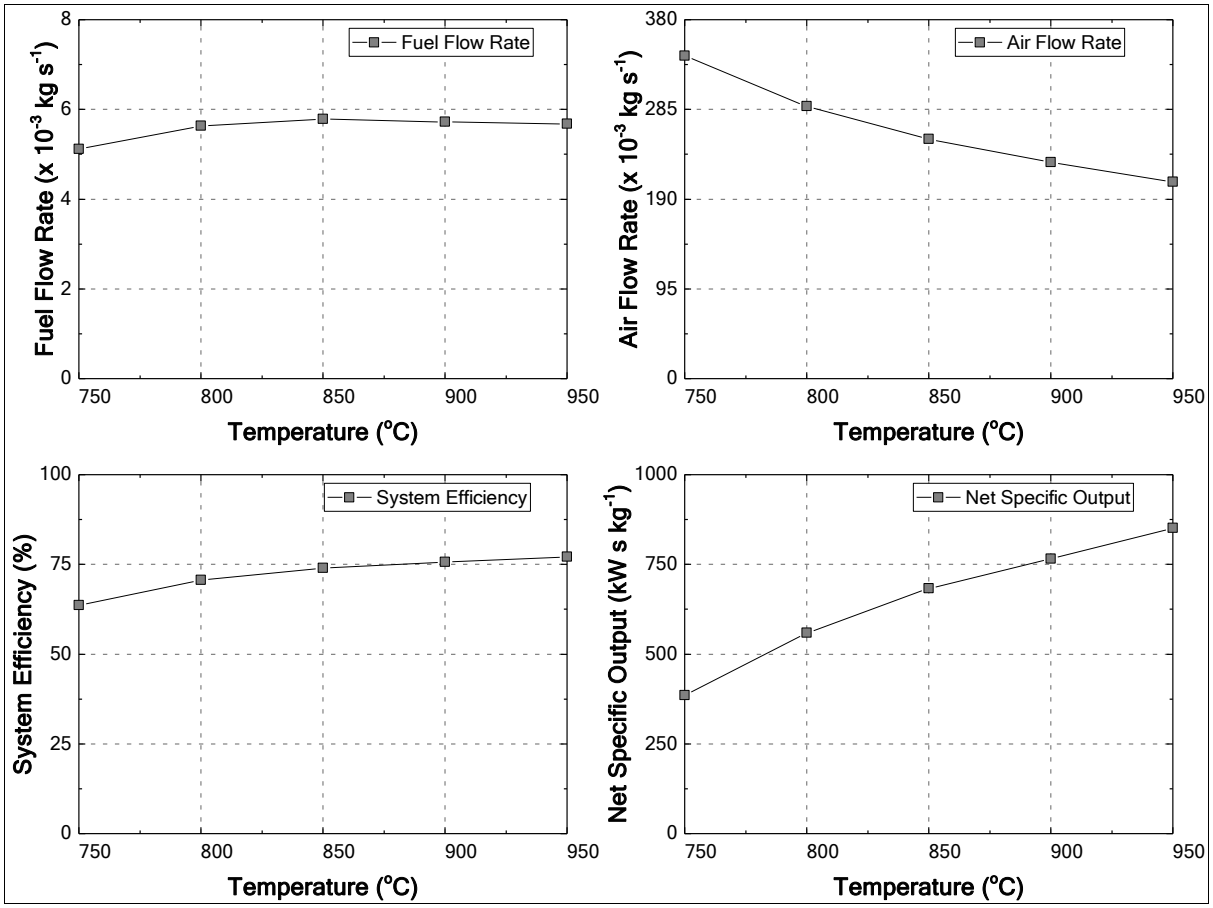

Figure 16. Trends in System Variables v/s Cell Temperature – Methane

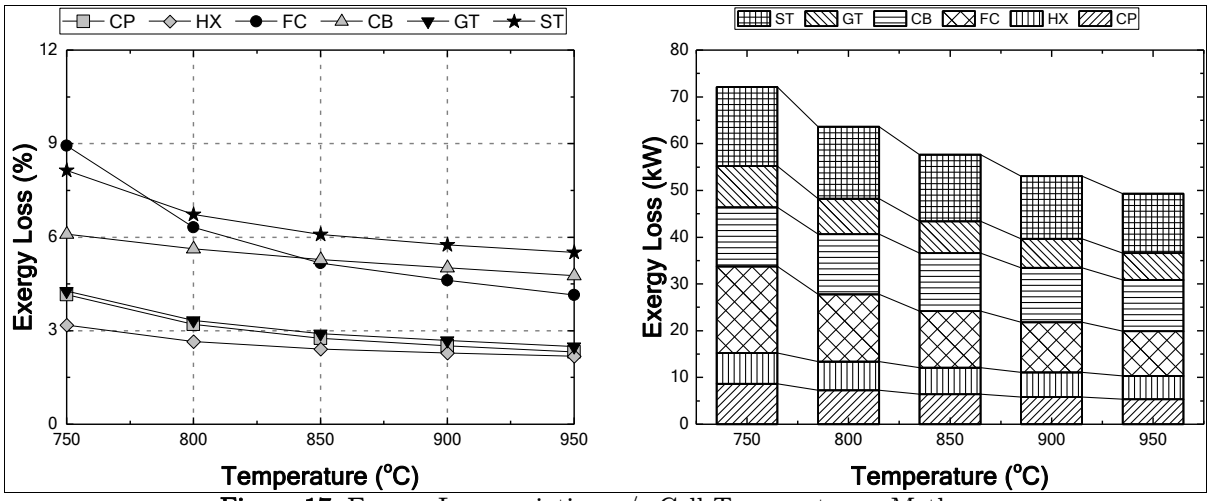

Figure 17. Exergy Loss variation v/s Cell Temperature - Methane

Pressure Ratio Variation

For the Methane model the pressure ratio was varied from 2-5.5 and the remaining parameters were taken from Table 1. As seen with the Hydrogen model, as the pressure ratio increases the turbine outlet temperature goes down (~10%) leading to a reduction in the

temperature of the fresh air stream after preheating (4.87%). At lower pressure ratios (2-2.5) there is sufficient heat available in the turbine exhaust to achieve the cell inlet temperature (900°C) in HX504 for fresh air. Therefore there is no air recirculation. At higher pressure ratios the fresh air temperature goes below 900°C and air recirculation gradually increases. This also implies that at pressure ratios below 3 the excess heat available results in a high ΔT_{high} in HX504 which leads to higher heat exchanger losses. Stack losses are also higher due to an increase in the stack temperature along with a higher air flow.

On the other hand, fresh fuel temperature remains practically constant since its maximum value (so the minimum fuel recirculation ratio) is mainly determined by carbon deposition safety. This value (about 850°C) is much lower than the turbine outlet temperature till a pressure ratio of 4.5 after which ΔT_{high} (30°C) in HX104 limits the maximum temperature achievable for the fresh fuel. At a pressure ratio of 5.5 the turbine outlet temperature drops to 872.8°C and as a result fresh fuel temperature drops to 842.5°C. Therefore fuel recirculation ratio remains almost constant till a pressure ratio of 5 and then increases sharply at 5.5. Variation of fuel and air flow rates with pressure ratio are shown in Figure 18

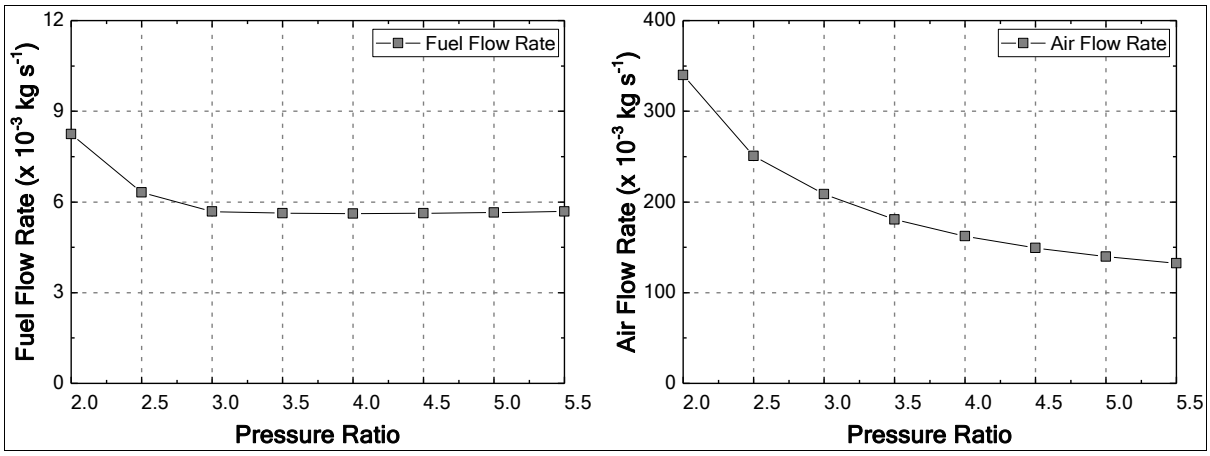

Figure 18. Fuel Flow, Air Flow v/s Pressure Ratio – Methane

An increasing specific output of the turbine leads to a reduction in the fresh air flow rate (61.1%). However the fuel cell efficiency only improves marginally at higher pressures as a result the turbine inlet temperature increases slightly (6.6%). This leads to a decrease in combustor, heat exchanger and compressor losses. Figure 19 presents the variation in exergy losses with pressure ratio.

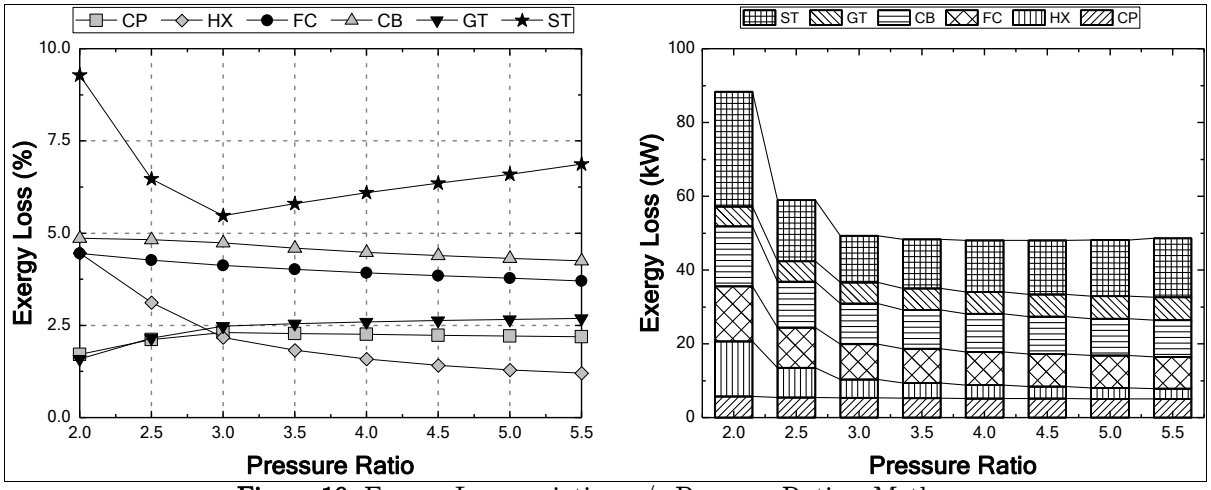

Figure 19. Exergy Loss variation v/s Pressure Ratio - Methane

Variations in system efficiency, specific output and specific fuel consumption are presented in Figure 20. System efficiency increases sharply (4.6%) till a pressure ratio of 3 and then becomes flat at higher pressure ratios. The optimum value for the pressure ratio is 5 above which it starts to decrease slightly and at even higher pressure ratios the decrease would become sharper. Specific fuel consumption curve is simply an inverted system efficiency curve. Specific output increases steadily in the considered range. Detailed explanations for these variations have been provided already in the Hydrogen section (pressure ratio variation) above.

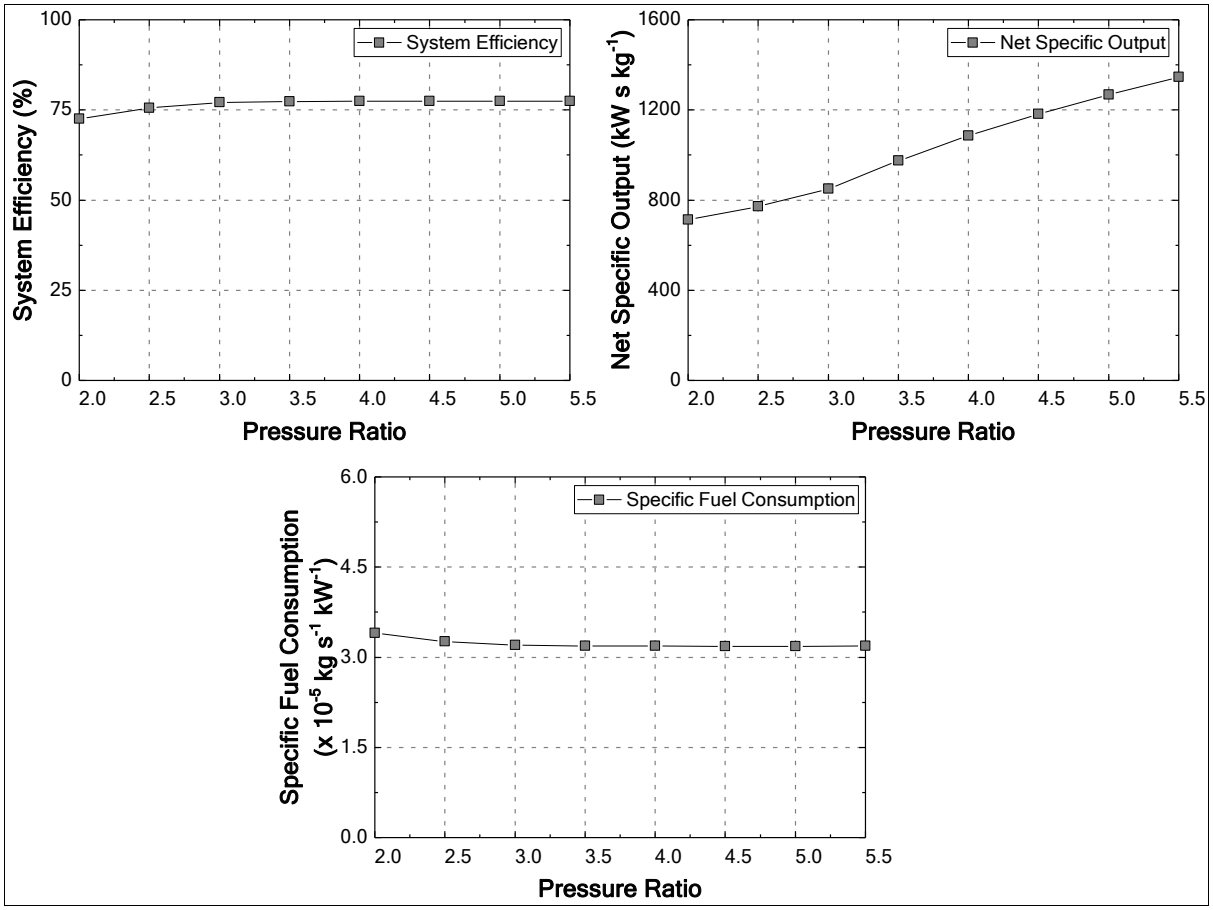

Figure 20. System Efficiency, Net Specific Output, Specific Fuel Consumption v/s Pressure Ratio – Methane

Fuel Utilization Variation

As explained in the Hydrogen section an increase in fuel utilization leads to an increase in fresh air flow rate (63.2%). With increasing utilization the amount of fuel (or LHV) left for the combustor goes down and a higher fuel flow is needed to generate the power specified in the gas turbine. However at fuel utilization below 85% the reduction in specific heat production in the cell is more significant since all the Methane in the fresh fuel is reformed (using up heat) but is not utilized. As a result even with a higher proportion of fuel being available to the combustor the fuel flow rate needs to be higher as the total heat flow to the gas turbine decreases significantly. Above 85% fuel flow increases as expected. Figure 21 presents the trends in system efficiency and other variables with fuel utilization.

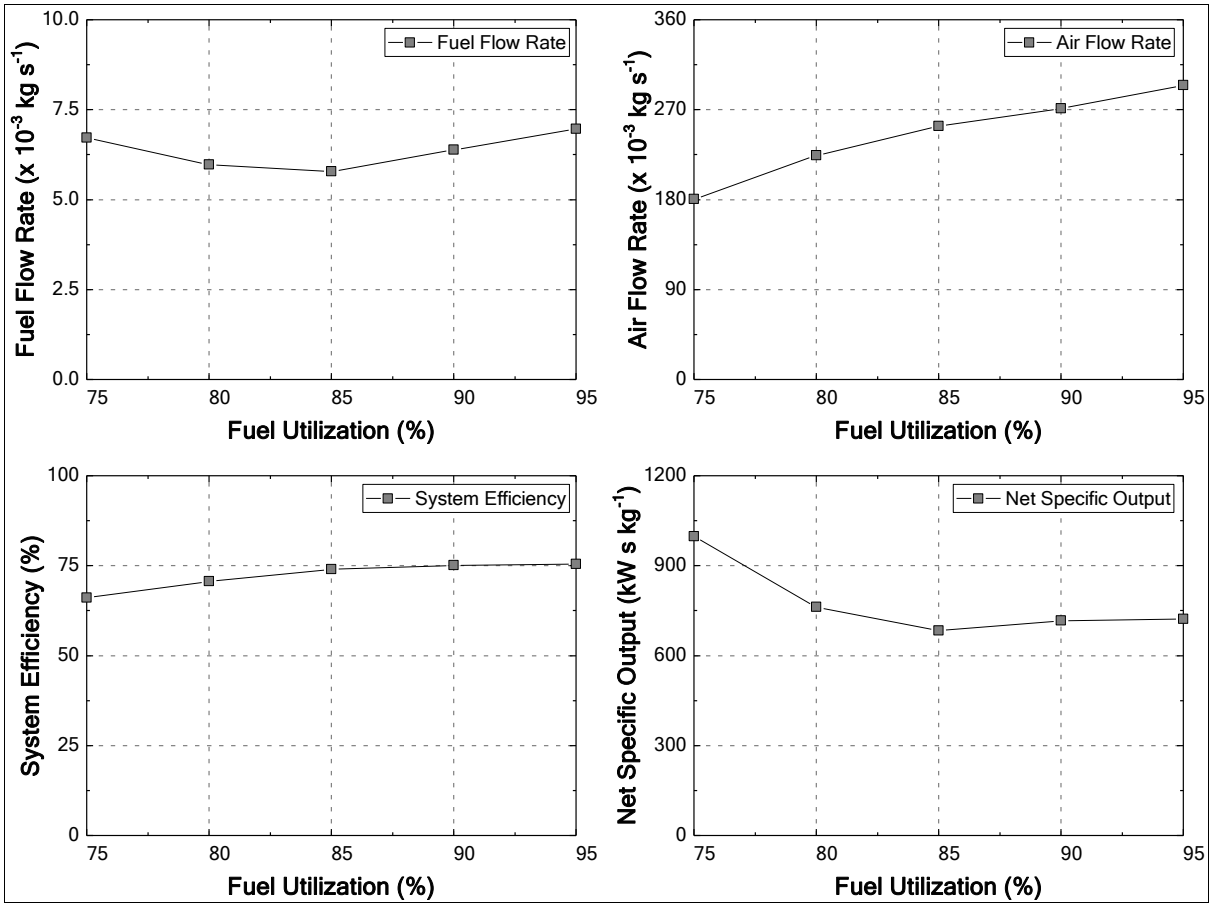

Figure 21. Trends in System Variables v/s Fuel Utilization – Methane

With increasing utilization turbine inlet and outlet temperatures go down and this is expected to lead to a decrease in the fresh air and fuel temperatures after preheating. Interestingly while the fresh air temperature after preheating does go down the fuel temperature goes up till a utilization of 90% and then decreases at 95%. This is due to the fact that the fresh fuel temperature is limited by the requirement of maintaining a certain fuel recirculation ratio in order to avoid carbon deposition at the cell inlet and not by a shortage of heat in the turbine exhaust (as verified by the high ΔT_{high} and ΔT_{low} in HX 104). As the utilization increases, the amount of steam in the anode exhaust increases and this allows the fuel recirculation ratio to be lowered (which is achieved by increasing the temperature of the fresh fuel at the outlet of HX 104) while still avoiding carbon deposition. At utilization rates above 90% temperature of the turbine exhaust becomes too low and the temperature of the fuel goes down, increasing the recirculation ratio as expected. At utilization rates lower than 85% there is enough heat in the turbine exhaust to bring the fresh fuel after HX504 itself to the cell inlet temperature thereby removing the need for cathode recirculation entirely. Exergy loss variations are presented in Figure 22.

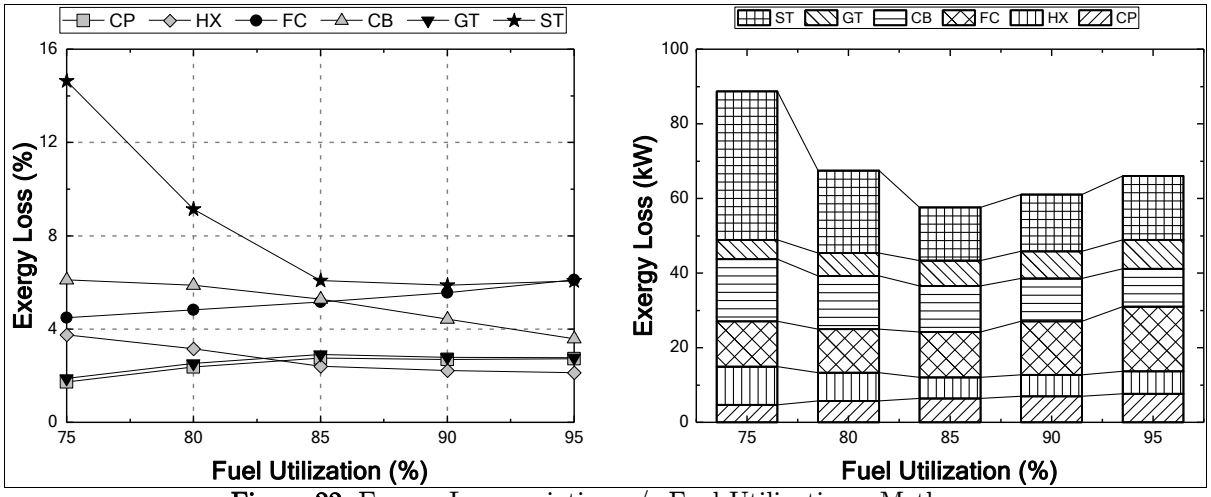

Figure 22. Exergy Loss variation v/s Fuel Utilization - Methane

3.4. Comparison of Hydrogen and Methane Models

In the sensitivity analysis sections certain differences were observed in the trends of exergy losses and the considered dependent variables. Reasons for these are explained below –

An increase in cell temperature leads to a reduction in all the losses with both Hydrogen and Methane. However in the case of Methane the combustor losses increase slightly (Figure 23) at a temperature of 800°C and then decrease even though due to a constantly decreasing air flow rate they are expected to decrease. This is due to the fact that the fuel flow rate increases rather strongly between 750-800°C (explained in the temperature variation section) which increases the input exergy to the combustor and therefore the losses.

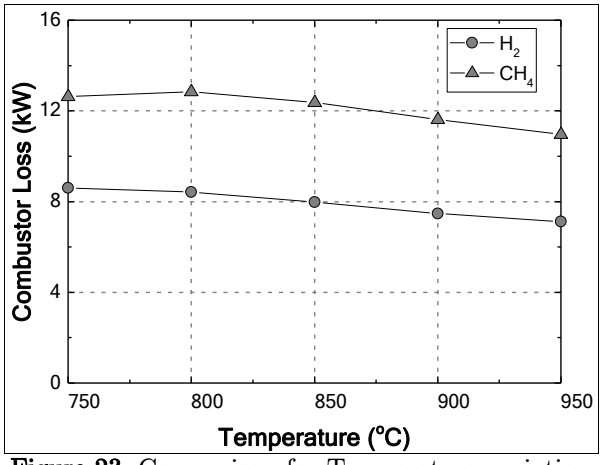

Figure 23. Comparison for Temperature variation

Increasing pressure ratio leads to a reduction in the air flow rate due to an increase in the specific output of the gas turbine and a slight improvement in the cell efficiency. As expected this leads to a reduction in the heat exchanger losses however in case of Methane these losses decrease more sharply from a pressure ratio of 2 to 2.5 as compared to Hydrogen. This is

also due to the fact that at pressure ratios 2 and 2.5 the amount of excess heat in the turbine exhaust (and consequently ΔT_{high} in HX504) is very high as the cell inlet temperature is already achieved after preheating. The same trend is also observed in stack losses which also decrease due to a decrease in the air flow rate. Combustor losses, which are expected to decrease due to a reduced air flow and increasing turbine inlet temperature (or combustor outlet temperature) start increasing slightly after a pressure ratio of 4.5 with Hydrogen. This is due to the fact that at higher temperatures the increase in exergy value of the flue gas due to increasing temperature is limited. Whereas the increase in fuel flow leads to a higher increase in exergy input to the combustor and therefore higher losses.

Compressor losses are expected to increase with pressure ratio due to higher entropy production at higher pressure ratios. However in the case of Hydrogen compressor losses decrease till a pressure ratio of 3 and then increase while for Methane they decrease over the whole range (Figure 24). Since specific compressor losses increase steadily for both Hydrogen and Methane it can be concluded that the compressor losses follow the variation in air flow rate. For Hydrogen the decrease in air flow rate from pressure ratio 2-3 is sharp but becomes flatter at higher pressure ratios (in comparison to Methane) and the increase in specific losses leads to an increase in total compressor losses.

The optimum pressure ratio for system efficiency was also found to be very different with Hydrogen and Methane. For practical regenerative gas turbine cycles it is known that higher turbine inlet temperatures lead to an increase in the optimum pressure ratio for system efficiency, while better heat exchanger effectiveness (or heat recovery from turbine exhaust) leads to a lower optimum pressure ratio [46]. With Methane the air factor is much lower as compared to Hydrogen and as a result the turbine inlet temperatures are higher by about 80-100 K. Due to the requirement of maintaining a minimum fuel recirculation in order to avoid carbon deposition (with Methane), the maximum possible fuel temperature after preheating is limited. As a result the heat available in the turbine exhaust cannot be recovered completely in the fuel preheater (HX104) as confirmed by high ΔT in HX104. So with Methane the optimum pressure ratio is higher due to higher turbine inlet temperature combined with lower heat recovery.

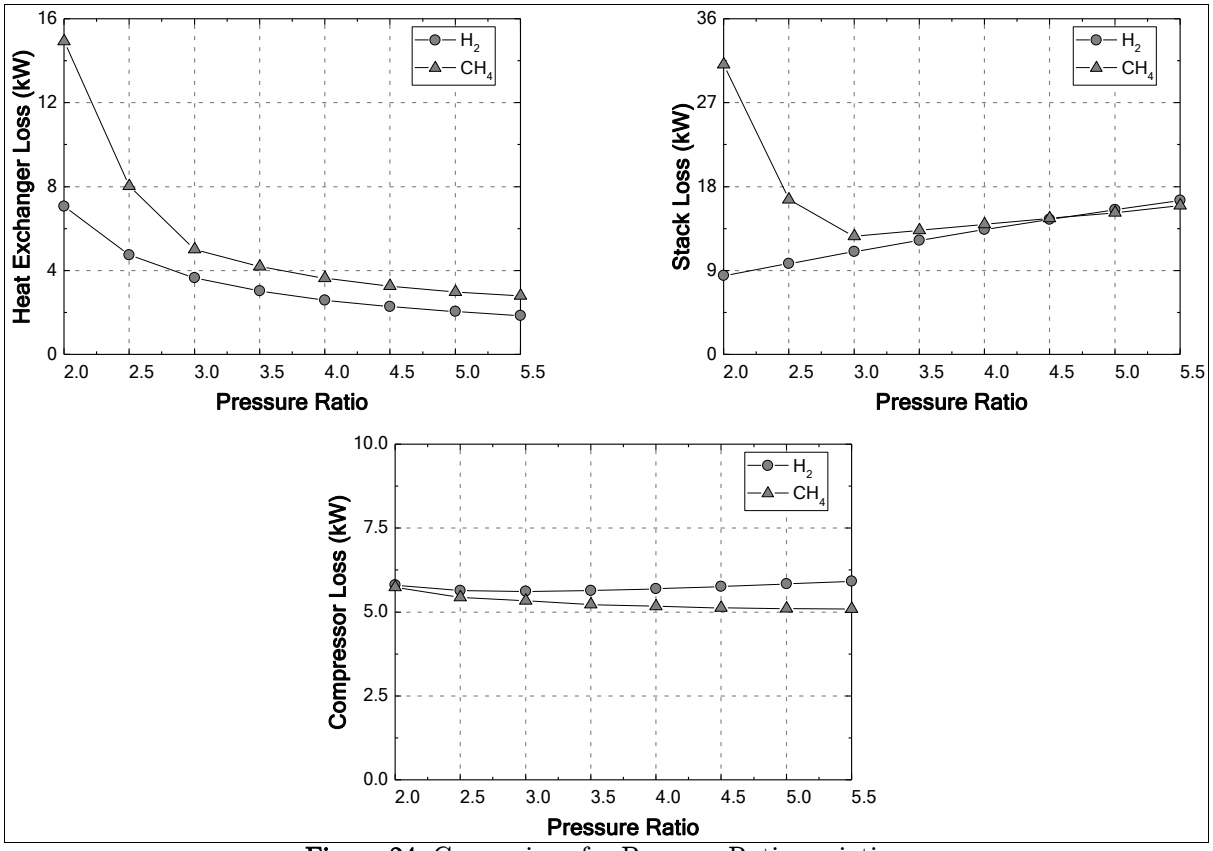

Figure 24. Comparison for Pressure Ratio variation

With increasing fuel utilization air flow rate in the systems increased due to an increase in the heat production in the cell which led to a steady increase in the heat exchanger losses (due to increasing transmitted heat). In the system with Methane however, the heat exchanger losses decrease between 75-85% utilization and then increase (Figure 25). This happens because with Methane turbine inlet and outlet temperatures are higher due to lower excess air flow. As a result temperatures of fresh air after the air preheater (HX504) are much closer to the cell inlet temperature as compared to Hydrogen. Thus at utilization rates below 85% fresh air gets completely heated to the cell inlet temperature in HX504 and ΔT_{high} increases (with decreasing fuel utilization) leading to an increase in heat exchanger losses. The increase in ΔT_{high} for fuel utilizations below 85% is made stronger by the lower air factor and higher fuel conversion in the combustor (which leads to higher temperatures after the combustor and the GT). As the heat left in the turbine exhaust increases it also leads to an increase in the stack temperature (and therefore stack losses). Whereas in the case of Hydrogen, stack losses decrease steadily from 85% to 75% utilization. When increasing fuel utilization fuel cell losses increase with Hydrogen but with Methane they decrease slightly from 75-80% and then increase. This is simply a result of the decreasing fuel flow rate till a utilization of 85% with Methane as specific fuel cell losses (w.r.t fuel flow rate) increase constantly.

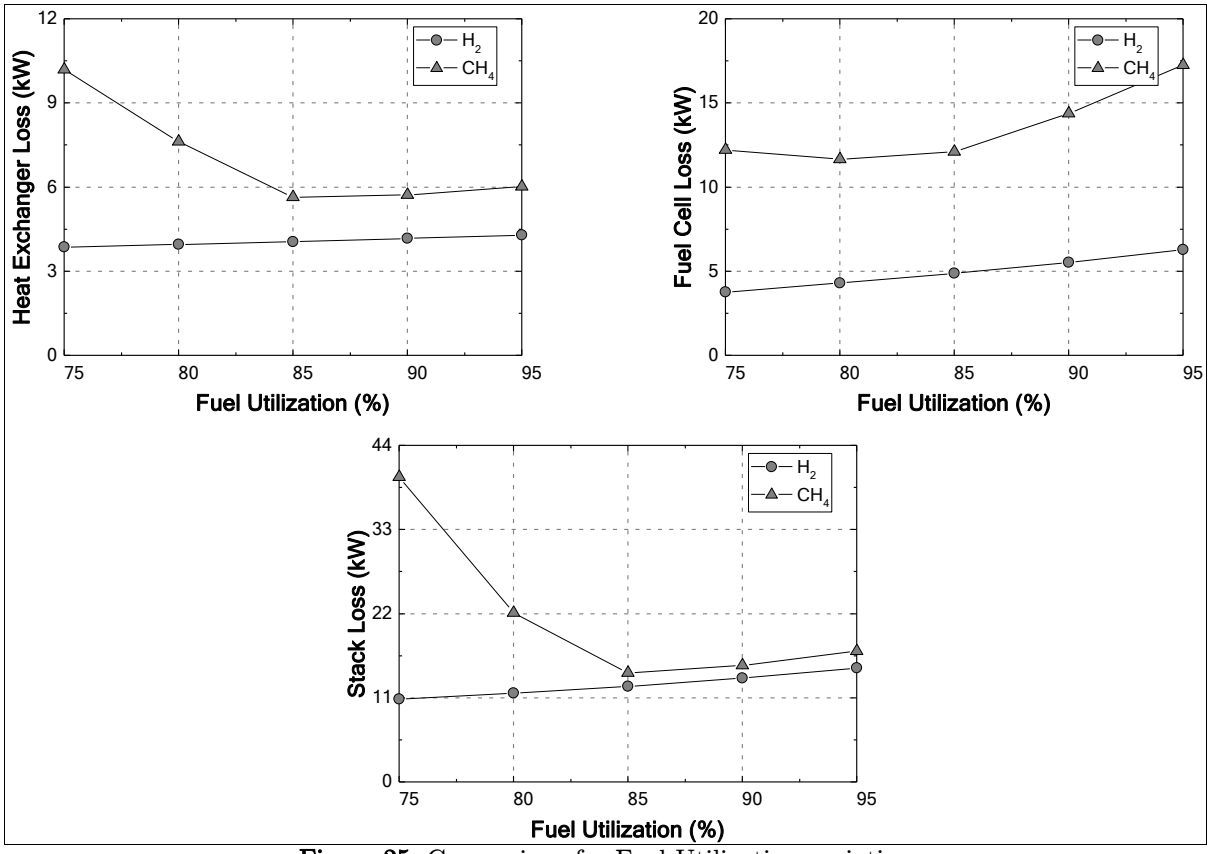

Figure 25. Comparison for Fuel Utilization variation

3.5. Conclusions

The objective of this chapter was to perform a sensitivity analysis to determine the impact of variation of the most important system parameters on key dependent variables and determine optimum values for these system parameters if any. Three parameters namely temperature, pressure ratio and fuel utilization were varied, with fuel flow rate, air flow rate, recirculation ratios and system efficiency being the monitored dependent variables. In addition exergy losses in various components were studied in order to gain a deeper understanding of the origins and behaviour of the losses with varying system parameters and utilize the results to improve system performance further.

Increasing cell temperature resulted in a decrease in all the exergy losses and system efficiency increased steadily with both Hydrogen and Methane. This increase in system efficiency follows mainly from the reduction in the cell resistance and can be expected to vary with the type of the fuel cell. The highest temperature considered (950°C) is therefore taken as the optimum value for further system optimization. With pressure ratio variation, the trends in different system variables (eg. Specific output, system efficiency) with both the fuels were found to be similar to that of a regenerative gas turbine cycle. Pressure ratios of 2.5 and 5 were found to be optimum with Hydrogen and Methane respectively. Pressure ratio as a parameter has been considered in previous system studies, however a detailed

comparison (along with explanations for the differences) for different fuels based on the same system configuration and constraints has not been reported before to the best of author's knowledge.

Increasing fuel utilization leads to an increase in all the losses except in the combustor but system efficiency is still found to increase steadily due to a higher fuel conversion in the fuel cell. Since fuel utilization above 85% is not encountered practically it is taken as the optimum value for both Hydrogen and Methane.

4

System Optimization

This chapter presents the steps undertaken to optimize the system efficiency with Hydrogen and Methane, utilizing the results from the sensitivity analysis chapter.

4.1. Hydrogen

From the base case results for the Hydrogen model we can see that the biggest loss making component in the system is the stack (8.8%) followed by the combustor (5.6%), gas turbine (4.7%) and the compressor (4.7%) while fuel cell (3.4%) and heat exchanger losses (2.9%) are the lowest. As explained in the sensitivity analysis section with increasing cell temperature all the losses decrease steadily with the fuel cell losses decreasing sharply. Gas turbine and stack losses increase with pressure ratio while the other losses decrease (compressor losses increase till a pressure ratio of 3 and then decrease). Stack losses increase significantly even though the air mass flow rate decreases due to a 37% increase in stack temperature. With increasing fuel utilization, fuel cell and stack losses increase while all the other losses decrease. Stack losses decrease due to a reduction in the air mass flow rate as the stack temperature remains almost constant.

These results show that the fuel cell itself is very efficient and the losses are because of excess air flow in the system which arises due to the absence of an internal heat sink in the fuel cell (reforming reaction). In order to improve the system efficiency it is necessary to reduce the amount of cooling air required by the fuel cell. Using the results of the sensitivity analysis the system with a cell temperature of 950^{0}C, pressure ratio of 2.5 and a fuel utilization of 85% is selected for further optimization. The results for the base model with these parameters are presented in Table 5 below.

Table 5. Base Case Results - Hydrogen (950°C, PR 2.5, UF 85%)

Parameter	Value
Exergy Efficiency	74.37%
Energy Efficiency	72.85%
Fuel Recycle Ratio	9.08
Air Recycle Ratio	0.48
Air Factor	34.47
Fuel Cell Power	76.3 kW
Per Pass Fuel Utilization	72.3%
Per Pass Air Utilization	9.92%

The series of steps undertaken to improve the system efficiency are described below -

Increasing the preheated fresh fuel temperature after heat exchanger 104

At a fixed temperature and fuel utilization, cell efficiency can be increased by ensuring that the fuel at the inlet is undiluted, which in the considered system means reducing fuel recirculation. Therefore as a first step ΔT_{high} in the heat exchanger 506 is increased from 30 to 37.77 °C this reduces the temperature of the fresh preheated air by about 6.6 °C and leaves more heat to be used for preheating the fresh fuel in the HX 104 where ΔT_{high} comes down from 150 to 30 °C and the temperature of the preheated fuel increases from 727.78°C to 848.97 °C (fuel recirculation ratio decreases from 9.08 to 2.71). System efficiency increases to 74.86% (energy efficiency 73.33%). Air factor in the combustor also comes down to 33.71 indicating a slight reduction in the excess air flow in the system. The exact value of ΔT_{high} in HX504 depends on the temperatures and flows in the system and needs to be adjusted accordingly so that both ΔT_{high} and ΔT_{low} in HX 104 are brought down to 30°C thereby maximizing the fresh fuel temperature and minimizing the heat transfer losses.

Removing fuel recirculation

To further reduce the air factor fuel recirculation is removed and the anode exhaust is used only to bring the preheated fuel to the cell inlet temperature. Fresh fuel composition is changed from 100% Hydrogen to a mix of 99% Hydrogen and 1% water. This introduces additional heat exchanger and pressure losses in the system but the reversible voltage at the inlet and consequently the operating voltage of the fuel cell also goes up (since the fuel composition with recirculation was 77.96% Hydrogen and 22.04% water) leading to lower heat production (due to higher efficiency) and thereby a reduction in the cooling air demand (air factor comes down to 33.43). The system efficiency goes up to 75.014% (energy efficiency 73.47%). At this point improving cell efficiency (without changing the resistance or the current density) or reducing excess air flow in the system by other means is not possible. Since the fuel utilization is very high the reversible voltage at the outlet of the cell and consequently the cell operating voltage suffers due to depletion of the fuel. If the same overall utilization is split over two fuel cells connected in series then the first cell could achieve a much higher voltage (and efficiency) as compared to the base model with the two improvements discussed (814.9 mV) and the second cell would operate at a slightly lower voltage thereby reducing the excess air flow (and increasing the system efficiency). Selimovic and Palsson [33] reported an improvement in fuel cell efficiency when using fuel cells in series (for a constant overall utilization) with both Hydrogen and Methane which was attributed to a lower variation of Nernst potential between the inlet and outlet. Their study also revealed an existence of an optimum utilization for the first cell for maximum efficiency. For a natural gas fed SOFC-GT system with pre reforming an improvement in system efficiency

when using fuel cells in series was also reported. However it was attributed to higher overall utilization with two cells due to better thermal balance between the fuel cells and the gas turbine.

Adding a second fuel cell in series

As the next configuration change a second fuel cell is added in series with the first one. An overall fuel utilization of 42.5% is set for both the cells (for a total utilization of 85%). A temperature rise of 50 ^{0}C (between the inlet and outlet of the cell) is specified for the first cell and targeted for the second cell (since outlet temperature of the second cell provides a necessary degree of freedom). It should be noted here that specification of temperature rise for the first cell while leaving the outlet temperature of the second cell free is purely a modeling choice. It is also possible to specify the inlet temperature of the first cell along with outlet temperature of the second cell. In this way the outlet temperature of the first cell would provide the degree of freedom and the second cell would determine the air flow in the system. Both the approaches are same in principle and the choice of either one has no impact on the results. Since the latter approach was expected to lead to a higher number of user specifications and calculation issues it was opted to continue with the first approach.

The first cell operates at 925^{0}C (inlet 900^{0}C, outlet 950^{0}C) and the second one at 975^{0}C (inlet 950^{0}C, outlet ~1000^{0}C). This leads to a system efficiency of 75.77% (energy efficiency 74.22%) and an air factor of 32.27.

Optimizing fuel utilization for both the cells

As the second cell is directly connected to the first one and the temperature rise has been fixed for the first cell the excess air flow required for cooling is determined by the heat production in the first cell. Therefore to lower the air factor further it is necessary to reduce the fuel utilization in the first cell which will lead to lower heat production and therefore a lower cooling demand. However since the outlet temperature of the second cell is free it will increase above 1000°C which may not be a limitation for existing fuel cells but is considered to be the upper limit ($\pm$ 1%) in this study. With reducing utilization therefore, the inlet and outlet temperatures of the first fuel cell must also be reduced by some amount (keeping the temperature rise constant) in order to limit the rising outlet temperature of the second cell. This in turn leads to a reduction in the operating temperatures of both the cells which leads to higher resistances and consequently a higher cooling demand and a higher air factor. The optimum utilization for the first cell is reached when the reduction in cooling demand due to lower utilization is balanced by an increase in the same due to higher resistance. In the present system an overall utilization of 34.5% for the first cell (50.5% for the second) with 875°C as cell inlet and 925°C as outlet temperature is found to be optimum, leading to a system efficiency of 76.17% (energy efficiency 74.61%) and an air factor of 31.73.

It is worth mentioning here that the second approach for modeling two cells in series would have led to the same optimum values for the cell temperatures and fuel utilizations, with the only difference being the sequence of steps required.

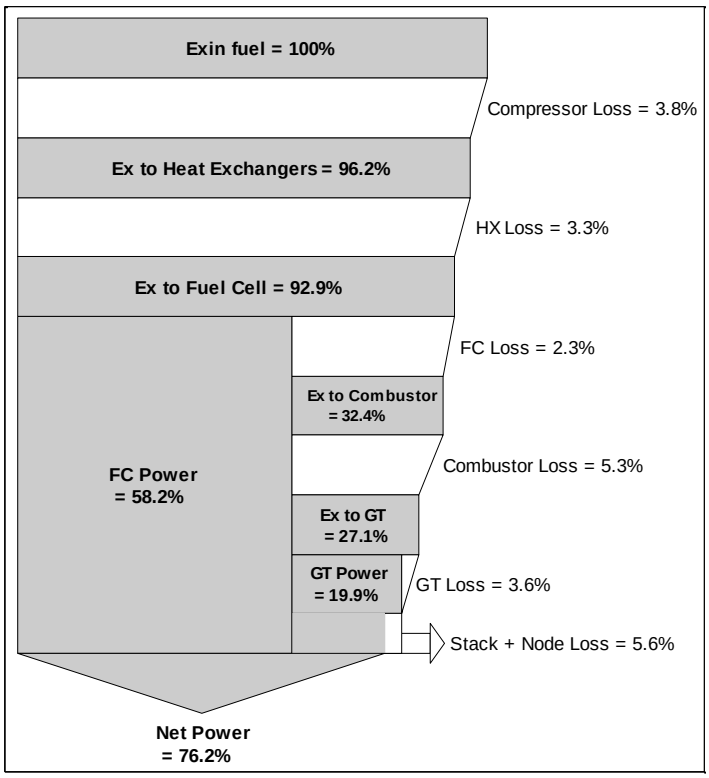

Figure 26. Exergy flow diagram – Hydrogen Optimized

Figure 26 presents the exergy flow diagram for the optimized case with Hydrogen. Table 6 presents the results for the optimized model. Due to the absence of fuel recirculation the overall and per pass fuel utilization values for the first cell are the same whereas they differ for the second cell.

Table 6. Optimized Case Results - Hydrogen

Parameter	Value
Exergy Efficiency	76.17%
Energy Efficiency	74.61%
Fuel Recycle Ratio	-
Air Recycle Ratio	0.12
Air Factor	31.73
Fuel Cell Power 1	37.3 kW
Fuel Cell Power 2	50.3 kW
Per Pass Fuel Utilization 1	34.50%
Per Pass Fuel Utilization 2	77.10%
Per Pass Air Utilization 1	5.59%
Per Pass Air Utilization 2	8.66%

4.2. Methane

The base case results for Methane reveal that the major losses are in the stack (6.08%), combustor (5.28%) and fuel cell (5.17%) while the heat exchanger, compressor and gas turbine losses are all below 3%. As with the Hydrogen model a decrease in cell temperature leads to a steady decrease in all the losses with the fuel cell loss being sharper. Similarly gas turbine and stack losses increase with pressure ratio. With increasing fuel utilization stack losses decrease significantly and start to increase very slightly at 95%. Fuel cell losses increase steadily while gas turbine and compressor losses increase between 75-85% and then become almost constant and heat exchanger losses decrease steadily between 75-85% and slowly afterwards.

The losses in the system are due to low fuel cell efficiency because of a lower fuel recycle ratio (therefore a higher per pass utilization) in comparison to Hydrogen (since less heat is required to preheat the fresh fuel to the cell inlet temperature). Excess air flow in the system is also minimal as indicated by an air factor of 15.93. Sensitivity analysis for Methane revealed optimum system performance at a pressure ratio of 5 and cell operating temperature of 950°C. Results for the base model with these parameters (and fuel utilization of 85%) are shown in Table 7 below followed by the steps taken to improve system efficiency.

Table 7. Base Case Results – Methane (950°C, PR 5, UF 85%)

Parameter	Value
Exergy Efficiency	77.50%
Energy Efficiency	80.39%
Fuel Recycle Ratio	1.06
Air Recycle Ratio	0.47
Air Factor	6.52
Fuel Cell Power	149.4 kW
Per Pass Fuel Utilization	81.44%
Per Pass Air Utilization	36.31%

Adding a second fuel cell in series and optimizing fuel utilization

Since fuel recirculation is already low and is necessary for prevention of carbon deposition it is not reduced further and the first step in order to improve fuel cell efficiency is to add another one. As with the Hydrogen model a fuel utilization of 42.5% was set for both the cells however that resulted in unacceptably high cell outlet (with carbon deposition at the inlet of the first cell) and turbine inlet temperatures, therefore the utilization in the first cell was increased (to increase the heat production) till 75.5% at which point an acceptable cell outlet temperature was achieved. Interestingly with increasing utilization in the first cell the system efficiency increases as well, even though the air factor increases. This again follows from the fact that low fuel cell efficiency itself causes high losses with Methane and not the

excess air flow rate. Therefore system efficiency goes up when a greater portion of the fuel is converted in the first cell as it operates at a higher efficiency but after a point this benefit is outweighed by a decrease in the efficiency of the second cell due to increasing fuel depletion. Increasing the utilization above 75.5% led to a decrease in the system efficiency therefore it is taken as the optimum. System efficiency of 78.01% (energy efficiency 80.92%) is achieved with an air factor of 5.75.

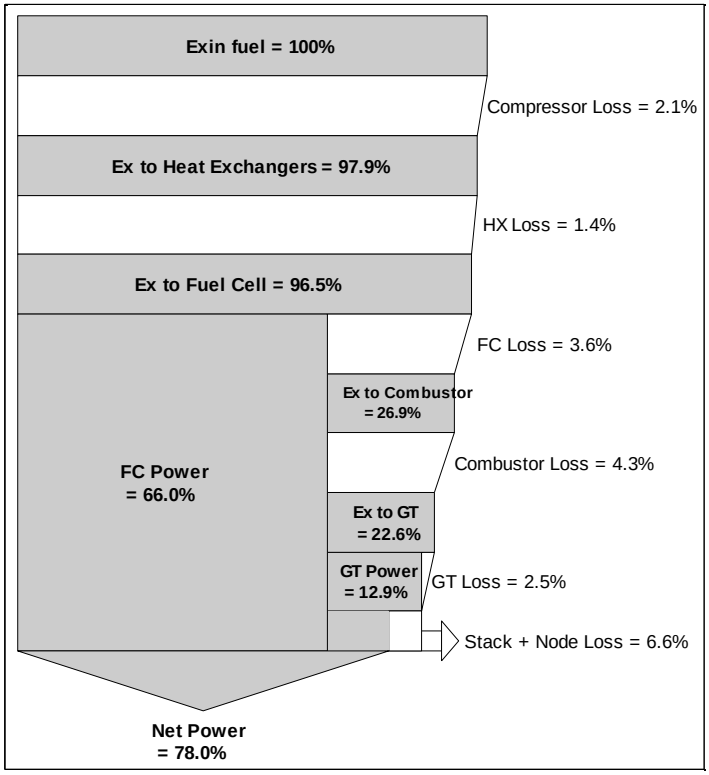

Figure 27. Exergy flow diagram – Methane Optimized

Figure 27 presents the exergy flow diagram for the optimized case with methane. Table 8 presents the results for the optimized model. It should be noted that the fuel utilization values presented in the table are *per pass* (for each cell) therefore they differ from the optimum utilizations discussed above (which were overall utilization values).

Table 8. Optimized Case Results - Methane

Parameter	Value
Exergy Efficiency	78.01%
Energy Efficiency	80.92%
Fuel Recycle Ratio	1.08
Air Recycle Ratio	0.17
Air Factor	5.75
Fuel Cell Power 1	131.1 kW
Fuel Cell Power 2	22.3 kW
Per Pass Fuel Utilization 1	68.78%
Per Pass Fuel Utilization 2	38.78%
Per Pass Air Utilization 1	37.86%
Per Pass Air Utilization 2	10.72%

4.3. Conclusions

The objective of this chapter was to utilize the results of the sensitivity analysis and identify the factors limiting system efficiency in case of Hydrogen and Methane and optimize the systems further. In the base configuration with Hydrogen the main limiting factor was found to be the excess air flow in the system with the fuel cell losses being the least significant. Therefore in order to improve system performance further strategies to reduce the air flow were devised. Two major configuration changes (removing fuel recirculation and addition of a second cell in series) along with two parameter optimizations (fresh fuel temperature and fuel utilization in the two cells) led to an increase in system efficiency from 74.37% to 76.17%.

With Methane the fuel cell itself was found to be the leading cause of high losses and therefore improvements to the cell efficiency were made by adding a second fuel cell in series and optimizing the utilizations for both. This resulted in an increase in system efficiency from 77.5% to 78.01%. Apart from the differences in the configuration changes made for Hydrogen and Methane another important difference was in the optimization of the fuel utilizations for the two cells. The optimum utilization for the first cell was found to be 34.5% in case of Hydrogen (leading to a slight increase in total fuel cell losses) while for Methane it was 75.5% (leading to lower total fuel cell losses). This follows from the difference in the limiting factors in both cases, which were excess air flow with Hydrogen and low fuel cell efficiency with Methane respectively.

5

System Modeling – No Gas Turbine

This chapter deals with system modeling and optimization results for an SOFC system without a gas turbine. The main hypothesis behind this study is that the heat being previously utilized in the bottoming cycle could be minimized and used completely for internal reforming of the fuel, which would lead to higher system efficiency. In addition to Hydrogen and Methane results are presented for Ammonia and Methanol as well since these fuels have been investigated more in SOFC system studies as compared to Hydrogen. A detailed analysis is presented for Hydrogen and Methane and based on the results conclusions are drawn for the other fuels.

5.1. Model Description

The proposed model (Figure 28) consists of a single SOFC followed by a combustor with its exhaust being used for preheating fresh air and fuel. Since the gas turbine is removed it is expected that a huge excess of heat will be available in the flue gas leaving the combustor and it will be sufficient to preheat the fresh fuel and air streams to the cell inlet temperature without the need for anode and cathode recirculation. Due to the absence of recirculation, fuel at the inlet is specified as 99% Hydrogen, 99% Ammonia, 49% Methane (in order to avoid carbon deposition) and 90% Methanol with the rest being water. For the base case cell parameters such as operating temperature, resistance and current density are taken from Table 1.

5.2. Base Case Results

Table 9 below presents the results for the base case model with Methane and Hydrogen.

Table 9. Base Case Results – No GT (850°C, UF 85%)

Parameter	Methane	Hydrogen	Ammonia	Methanol
Exergy Efficiency	56.99 %	48.52 %	52.87 %	48.71 %
Energy Efficiency	59.11 %	47.52 %	56.45 %	52.00 %
Air Factor	23.63	62.97	31.83	42.35
Fuel Cell Power	100 kW	100 kW	100 kW	100 kW
Per Pass Fuel Utilization	85.00 %	85.00 %	85.00 %	85.00 %
Per Pass Air Utilization	19.34 %	8.26 %	15.11 %	11.80 %

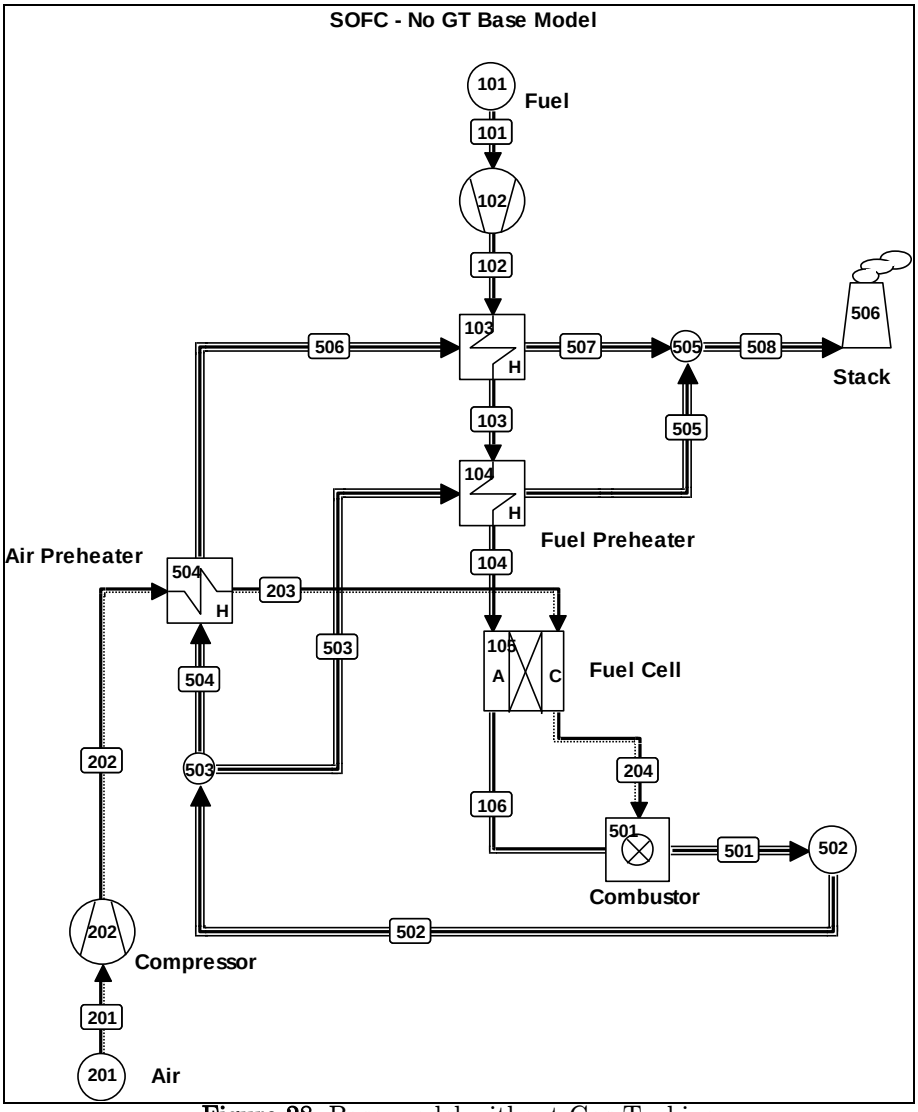

Figure 28. Base model without Gas Turbine

As expected, due to the absence of a bottoming cycle there is a lot of excess heat left in the system which leads to very high stack and heat exchanger losses. There are two sources of heat production in the system, the fuel cell and the combustor. Heat production within the cell has two sources, the exothermic electrochemical reactions ($T\Delta S$) and the ohmic losses (i^2R). An analysis of the results (shown in Figure 29) shows that heat production due to exothermic electrochemical reactions accounts for about 30.36% of the total heat production with Methane and 56.72% with Hydrogen (due to the lack of endothermic reforming reactions). It should be noted here that $T\Delta S$ in this study refers to the net heat production due to exothermic electrochemical reactions, i.e. the heat of endothermic reforming is subtracted.

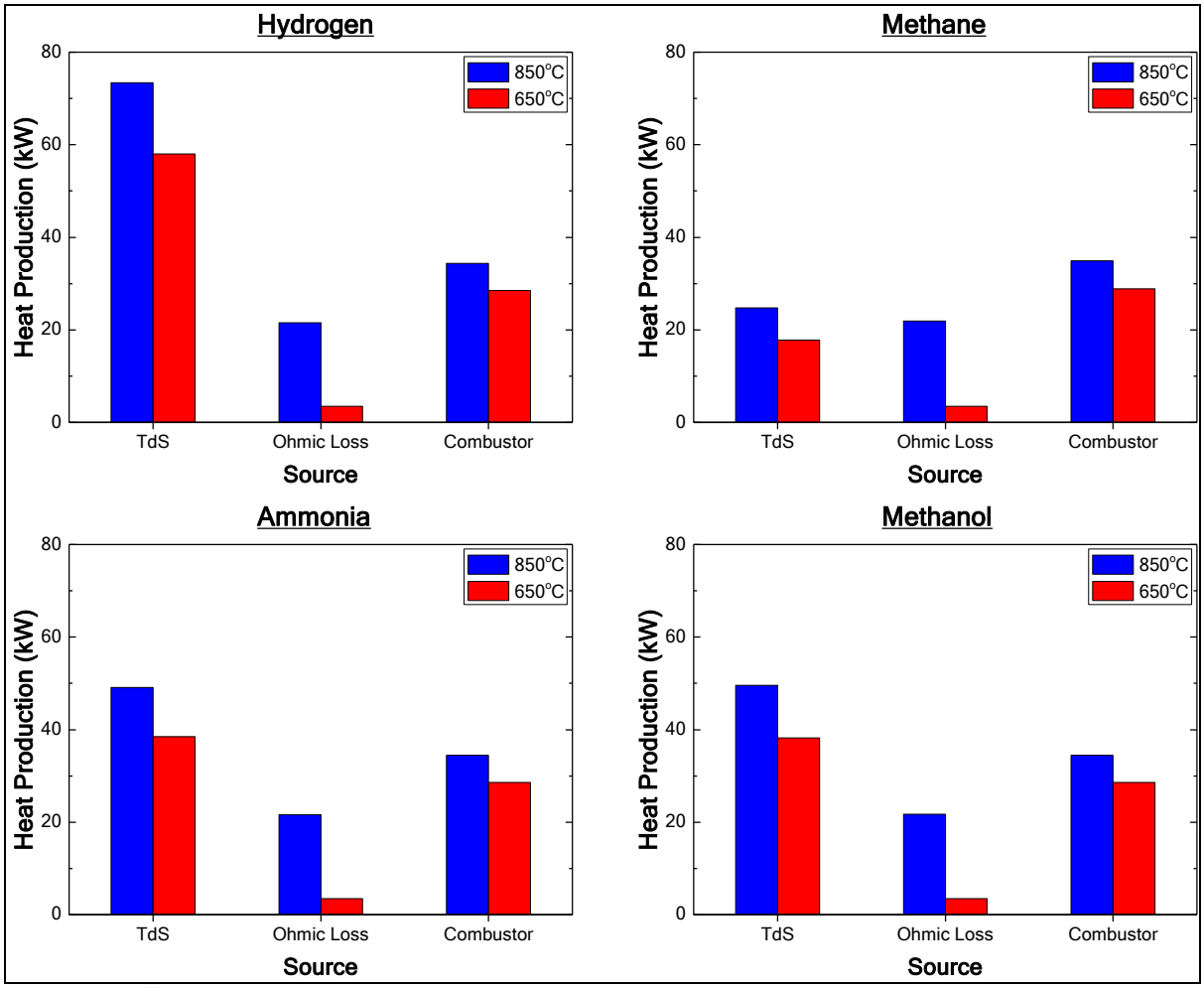

Figure 29. Heat Production distributions for all fuels at different temperatures

5.3. System Optimization

In CHP applications achieving overall system efficiencies of 80% or higher is possible with the considered base case system, however in order to improve the electrical efficiency it is necessary to reduce the heat production in the system. This can be done by improving the fuel utilization in the cell or by reducing the heat production within the cell itself. For a single cell fuel utilizations higher than 85% are unheard of. Cell efficiency can be improved to a certain extent by using two or more cells in series and setting total fuel utilization higher than 85% but that introduces a difficulty in controlling the temperature rise across individual cells and increases complexity in the system. Another option is to target the ohmic losses and $T\Delta S$. While ohmic losses can be reduced by lowering the resistance of the cell, $T\Delta S$ is dependent on the electrochemical reactions taking place and can only be reduced by using a fuel which has a high heat of reforming per mole of Hydrogen produced or by lowering the operating temperature of the cell. Among carbonaceous fuels Methane appears to have the highest heat of reforming therefore lowering the cell operating temperature is the only option left to reduce heat production in the cell. In case of Hydrogen a complete lack of

reforming reactions means that the operating temperature needs to be much lower to achieve similar efficiencies. As seen from Table10 the heats of reforming per mole of Hydrogen produced (with water gas shift) for Ammonia and Methanol lie in between those of Hydrogen and Methane. Therefore the heat production in the system with Ammonia and Methanol can also be expected to lie between Hydrogen and Methane. For this reason a detailed discussion of the results is only presented for Hydrogen and Methane.

Table 10. Heats of Reforming (850°C)

Parameter	Methane	Ammonia	Methanol
ΔHr (kJ/mol) per mole H_2	75.61	37.08	52.65
ΔHr (kJ/mol) per mole H_2 with WGS	48.33	37.08	23.93

Reducing cell operating temperature and resistance

In order to improve the electrical efficiency the cell operating temperature is reduced to 650°C and the resistance value (0.126 Ω-cm^2) from novel low temperature SOFCs [52] is used. Table 11 below presents the results for all the fuels. System efficiency in case of Methane increases by 13.67% and 12.1% in case of Hydrogen.

Table 11. Optimized Results – No GT (650°C, UF 85%)

Parameter	Methane	Hydrogen	Ammonia	Methanol
Exergy Efficiency	70.66 %	60.62 %	65.30 %	60.60 %
Energy Efficiency	73.29 %	59.37 %	69.71 %	64.71 %
Air Factor	3.4	42.46	11.55	22.06
Fuel Cell Power	100 kW	100 kW	100 kW	100 kW
Per Pass Fuel Utilization	85.00 %	85.00 %	85.00 %	85.00 %
Per Pass Air Utilization	62.53 %	11.78 %	32.92 %	20.44 %

The results show that this reduction in cell resistance and operating temperature leads to a significant reduction in the ohmic losses which decrease by 83.98% and 84.06% for Methane and Hydrogen respectively. For Methane at 850°C TΔS represents 30.36% of the total heat production in the system while combustor losses represent 42.76%. With a decrease in temperature this distribution becomes 35.43% and 57.57% respectively. On the other hand, for Hydrogen TΔS (56.72%) is much higher than combustor losses (26.60%) at 850°C and with a decrease in temperature the distribution does not change much (58.03% TΔS, 31.67% combustor losses).

Table 12. Heat Production Distributions (650°C, UF 85%)

Source	Methane	Hydrogen	Ammonia	Methanol
TΔS	17.77 kW	58.03 kW	38.47 kW	38.21 kW
Ohmic losses	3.51 kW	3.44 kW	3.45 kW	3.46 kW
Combustor	28.88 kW	28.49 kW	28.63 kW	28.60 kW

Increasing fuel utilization

To understand the effect of improving fuel utilization in detail it is increased from 85% to 90% (at 650°C) for both Hydrogen and Methane. For Hydrogen as expected, combustor losses decrease in both absolute (35.77%) and relative terms since a lower amount of fuel is combusted for the same power output. Ohmic losses increase insignificantly due to a slight increase in the cell area (so the total current drawn). TΔS increases (5.45%) as well due to higher amount fuel being converted in the cell. Due to the decrease in combustor losses being stronger the overall heat production in the system goes down by 7.73% and system efficiency increases to 62.71%.

With Methane while an increase in fuel utilization leads to a 36.46% decrease in combustor losses (absolute), TΔS increases by 21.33%. This still leads to a decrease in the overall heat production in the system by 13.24% and consequently the system efficiency increases to 73.64%. The changes in absolute losses are similar for Methane and Hydrogen.

As compared to the improvement in system efficiency with a reduction in temperature, an increase in fuel utilization leads to a small improvement. This is due to the fact that while heat production in the combustor goes down with increasing utilization, there is an increase in TΔS. A further increase in cell efficiency by adding a second cell in series or by increasing the overall utilization above 85% will therefore lead to an even lower improvement in efficiency.

5.4. Conclusions

The aim of this chapter was to determine whether acceptable system efficiencies (electrical) can be achieved with SOFCs without the use of any bottoming cycle. It is found that the removal of the gas turbine leads to a low system efficiency as a large excess of heat is lost as stack losses. In order to improve the efficiency the objective then becomes to minimize heat production in the system. The fuel cell and combustor are identified as the only heat producing components in the system. Lowering the cell operating temperature along with the cell resistance is found as a possible solution to reduce fuel cell losses.

Combustor losses are reduced to an extent by improving the cell efficiency but for further reduction, fuel utilization needs to be increased. Increasing fuel utilization reduces combustor losses but increases fuel cell losses at the same time which limits the increase in system efficiency. Therefore in order to gain the true benefit of increasing fuel utilization it is important to reduce the cell operating temperature at the same time. The required decrease in temperature depends on the distribution of heat production between the combustor and the fuel cell, which depends on the type of fuel.

With Hydrogen it is found that the absence of endothermic reforming reactions leads to extremely high heat production (73.36% of the total heat production) in the cell which can only be reduced by reducing the cell operating temperature. Increasing fuel utilization is found to have a positive effect on the efficiency. However even with these optimizations the efficiency achieved is very low and it is concluded that the operating temperature needs to be lowered drastically to about 250-350°C in order to achieve high efficiencies with Hydrogen as a fuel.

Acceptably high efficiencies are obtained with Methane at 650°C with scope for a significant increase by a reduction in the operating temperature to 550-600°C (provided that internal reforming can be achieved at these low temperatures) along with the use of two or more cells in series. The efficiency obtained with Ammonia is higher than Hydrogen but less than Methane. However with a further reduction in cell temperature and increase in utilization it can be an interesting choice as a fuel. The exergy efficiency obtained with Methanol is slightly lower than Hydrogen but the energy efficiency is higher but still lower in comparison to Ammonia. Cell temperatures of around 450°C might make Methanol a viable option as well.

6

Conclusions and Future Work

6.1. Conclusions

Sensitivity analysis for the base configuration with Hydrogen and Methane revealed that increasing fuel cell operating temperature has a positive effect on the system efficiency and all the component losses. High efficiencies are obtained with high cell operating temperatures and higher temperatures can be expected to lead to higher efficiencies. The improvement in electrical efficiency from 59.25% to 72.39% (with Hydrogen) and 65.99% to 80.01% (with Methane) can be attributed to the strong decrease in cell resistance with increasing temperature therefore the variation in system efficiency for different cells is expected to follow the behaviour of cell resistance with temperature and if similar cell resistances can be obtained at lower temperatures, comparable efficiencies may be achieved at lower temperatures as well. System efficiency increased throughout in the considered temperature range of 750-950°C.

Higher efficiencies are also obtained at high fuel utilizations as the proportion of power produced by the fuel cell increases. It is concluded that the highest possible utilization would lead to highest system efficiencies even though the fuel cell efficiency itself reduces. In the considered range (75-95%) the system efficiency increased and started to become flatter but an optimum value was not observed.

A flat but very different optimum for pressure ratio is observed with both Hydrogen (2.5) and Methane (5) as expected for a practical regenerative gas turbine cycle. The optimum pressure ratio is higher with Methane due to higher turbine inlet temperatures and poorer heat exchanger effectiveness (more precisely heat recovery). Although pressure ratio as a parameter has been considered in previous system studies, the comparison for different fuels especially with a strong thermodynamic basis has not been studied before to the best of author's knowledge.

An assessment of sensitivity analysis results also reveals that fuel recirculation ratio and air recirculation ratio are mainly determined by the heat production in the fuel cell. Air flow rate is determined jointly by the gas turbine and the cooling demand in the fuel cell. In the

case of Methane the endothermic reforming reaction reduces the specific heat production in the cell which reduces the amount of fresh air flow in the system. This reduction in the air flow rate eventually leads to lower fuel recirculation ratios and a lower proportion of power produced by the turbine which results in higher system efficiency. Therefore it can be concluded that fuels which can be internally reformed (such as methanol, ethanol) in the SOFC will have an advantage of better heat utilization in the system and the higher the heat of reforming per mole of Hydrogen produced (with water gas shift reaction) the higher will be the system efficiency.

In the case of Hydrogen excess air flow rate was found to be the cause of high exergy losses in all the components, which were minimized by removing anode recirculation and adding a second fuel cell in series with the first one. In this modified configuration system efficiency was found to be highly dependent on the fuel utilization rates to be specified in both the cells and an interesting tradeoff emerged between increasing fuel cell losses (by reducing the utilization in the first cell) and improving system efficiency (due to reducing excess air flow rate).

Since fuel cell losses actually increase (by reducing the utilization in the first cell) it can be concluded that the improvement in the system efficiency (or the reduction in excess air flow) follows from the higher temperature rise across the two fuel cells (~125 K as opposed to 100 K in the base model). In the present study this temperature rise was limited by the maximum cell outlet, turbine inlet temperature and the high cell resistance at lower temperatures. With SOFCs that can achieve a low enough resistance at lower temperatures or operate at still higher temperatures, this temperature rise can be increased and system efficiency will go up further. Electrical efficiency of 74.61% (system exergy efficiency 76.17%) was achieved with the optimized model.

With Methane mainly fuel cell losses caused low system efficiency therefore adding another cell in series and maximizing the utilization in the first cell (in contrast to Hydrogen) led to an improvement in the system efficiency. For the optimized model an electrical efficiency of 80.92% (system exergy efficiency 78.01%) was achieved.

Reasonably high electrical efficiency of 73.29% (system exergy efficiency 70.66%) was achieved without the use of a gas turbine with Methane as a fuel and low temperature (650°C) fuel cells. The high efficiency is attributed to the minimization of the heat left after the SOFC and its utilization for internal reforming of the fuel. As compared to the SOFC-GT system fueled by Methane the efficiency achieved without the gas turbine is much lower (about 7.4%). However this system can certainly be considered for applications where space and weight are limitations such as marine applications or aircraft APUs. It is also noted that this efficiency is based on the assumption that internal reforming is also possible with these low temperature fuel cells.

To summarize –

- Comparable system exergy efficiencies can be obtained with different fuels when the system configuration is optimized accordingly
- Electrical efficiencies (net power) of 74.61% and 80.92% are obtained with Hydrogen and Methane respectively
- High efficiencies are obtained at high cell operating temperatures and fuel utilizations
- Very different optimum pressure ratios of 2.5 and 5 are obtained for Hydrogen and Methane respectively
- Reasonably high electrical efficiencies (73.29%) are obtained without a gas turbine with Methane
- Complex system configurations may not be needed for achieving comparable electrical efficiencies with SOFCs fed on Ammonia and Methanol as well

6.2. Future Work

When connecting cells in series controlling the temperature rise across individual cells becomes difficult. Bypassing an amount of fresh air and supplying it at the inlets of successive cells could lead to better temperature control and efficiency. It can also be interesting to use a low temperature SOFC followed by intermediate and high temperature SOFCs with certain fractions of fresh fuel supplied at the inlet of each cell. As far as fuel cell efficiency is concerned (or systems where fuel cell losses are the major loss making components) it is seen that operating successive cells at higher temperatures may be beneficial for electrical efficiency since fuel depletion leads to lower Nernst voltages and that might be compensated by a lower cell resistance at higher temperatures. For systems where fuel cell efficiency itself is high (such as with Hydrogen in the present study) operating successive cells at the same temperature by employing cooling in between cells could be beneficial for system efficiency.

Although with Hydrogen a high efficiency is achieved in the optimized configuration it can be seen that the air factor is still very high (31.73) and could be reduced further by increasing the temperature rise across the cells and needs to be investigated further. Influence of adding more than two cells on the system efficiency with both Hydrogen and Methane should also be studied. With Methane there is a scope for optimization of the fuel composition. Reducing the proportion of Methane in the fresh fuel would allow fuel recirculation to be reduced further however doing so implies utilizing more heat at a lower temperature in the preheater and could lead to lower system efficiencies. Varying current density simply represents a tradeoff between capital and operating costs but may have an impact on the optimum system parameters determined in this study and is therefore along with other points recommended as future work. As comparable system efficiencies are

obtainable with different fuels (when optimized accordingly), the study needs to be extended to other biofuels and the scope should be increased to include the processes involved in the production of these fuels from their respective sources. Such a study will help in bringing clarity about the choice of the energy carrier for future systems.

Bibliography

1. Choudhury, A., H. Chandra, and A. Arora, *Application of solid oxide fuel cell technology for power generation—A review.* Renewable and Sustainable Energy Reviews, 2013. **20**: p. 430-442.
2. Eguchi, K., et al., *Fuel flexibility in power generation by solid oxide fuel cells.* Solid State Ionics, 2002. **152**: p. 411-416.
3. Buonomano, A., et al., *Hybrid solid oxide fuel cells–gas turbine systems for combined heat and power: A review.* Applied Energy, 2015. **156**: p. 32-85.
4. Zhang, X.W., et al., *A review of integration strategies for solid oxide fuel cells.* Journal of Power Sources, 2010. **195**(3): p. 685-702.
5. Varbanov, P. and J. Klemes, *Analysis and integration of fuel cell combined cycles for development of low-carbon energy technologies.* Energy, 2008. **33**(10): p. 1508-1517.
6. Rao, A.D. and G.S. Samuelsen, *A thermodynamic analysis of tubular solid oxide fuel cell based hybrid systems.* 2003.
7. Eveloy, V., et al., *Energy, exergy and economic analysis of an integrated solid oxide fuel cell–gas turbine–organic Rankine power generation system.* International Journal of Hydrogen Energy, 2016.
8. Shiratori, Y., et al., *Application of Biofuels to Solid Oxide Fuel Cell.* ECS Transactions, 2011. **35**(1): p. 2641-2651.
9. Hong, W.T., et al., *Efficiency analyses of ethanol-fueled solid oxide fuel cell power system.* Applied Energy, 2011. **88**(11): p. 3990-3998.
10. Liso, V., et al., *Solid oxide fuel cell performance comparison fuelled by methane, MeOH, EtOH and diesel surrogate C8H18.* Applied Thermal Engineering, 2015.
11. Fernandes, A., T. Woudstra, and P.V. Aravind, *System simulation and exergy analysis on the use of biomass-derived liquid-hydrogen for SOFC/GT powered aircraft.* International Journal of Hydrogen Energy, 2015. **40**(13): p. 4683-4697.
12. Wojcik, A., et al., *Ammonia as a fuel in solid oxide fuel cells.* Journal of Power Sources, 2003. **118**(1-2): p. 342-348.
13. Douvartzides, S., F. Coutelieris, and P. Tsiakaras, *Exergy analysis of a solid oxide fuel cell power plant fed by either ethanol or methane.* Journal of Power Sources, 2004. **131**(1): p. 224-230.
14. Laosiripojana, N. and S. Assabumrungrat, *Catalytic steam reforming of methane, methanol, and ethanol over Ni/YSZ: The possible use of these fuels in internal reforming SOFC.* Journal of Power Sources, 2007. **163**(2): p. 943-951.
15. Demirbas, M.F., M. Balat, and H. Balat, *Potential contribution of biomass to the sustainable energy development.* Energy Conversion and Management, 2009. **50**(7): p. 1746-1760.
16. Ho, D.P., H.H. Ngo, and W. Guo, *A mini review on renewable sources for biofuel.* Bioresource Technology, 2014. **169**: p. 742-749.
17. Vassilev, S.V., C.G. Vassileva, and V.S. Vassilev, *Advantages and disadvantages of composition and properties of biomass in comparison with coal: An overview.* Fuel, 2015. **158**: p. 330-350.

18. Demirbas, A., *Potential applications of renewable energy sources, biomass combustion problems in boiler power systems and combustion related environmental issues.* Progress in Energy and Combustion Science, 2005. **31**(2): p. 171-192.

19. Kuchonthara, P., S. Bhattacharya, and A. Tsutsumi, *Energy recuperation in solid oxide fuel cell (SOFC) and gas turbine (GT) combined system.* Journal of Power Sources, 2003. **117**(1-2): p. 7-13.

20. Granovskii, M., I. Dincer, and M.A. Rosen, *Performance comparison of two combined SOFC–gas turbine systems.* Journal of Power Sources, 2007. **165**(1): p. 307-314.

21. Ma, S., et al., *Thermodynamic analysis of a new combined cooling, heat and power system driven by solid oxide fuel cell based on ammonia–water mixture.* Journal of Power Sources, 2011. **196**(20): p. 8463-8471.

22. Zhao, Y., N. Shah, and N. Brandon, *Comparison between two optimization strategies for solid oxide fuel cell–gas turbine hybrid cycles.* International Journal of Hydrogen Energy, 2011. **36**(16): p. 10235-10246.

23. Akkaya, A.V., B. Sahin, and H.H. Erdem, *An analysis of SOFC/GT CHP system based on exergetic performance criteria.* International Journal of Hydrogen Energy, 2008. **33**(10): p. 2566-2577.

24. Haseli, Y., I. Dincer, and G.F. Naterer, *Thermodynamic modeling of a gas turbine cycle combined with a solid oxide fuel cell.* International Journal of Hydrogen Energy, 2008. **33**(20): p. 5811-5822.

25. Motahar, S. and A.A. Alemrajabi, *Exergy based performance analysis of a solid oxide fuel cell and steam injected gas turbine hybrid power system.* International Journal of Hydrogen Energy, 2009. **34**(5): p. 2396-2407.

26. Haseli, Y., *Optimum Performance of a Regenerative Gas Turbine Power Plant Operating With/Without a Solid Oxide Fuel Cell.* Journal of Fuel Cell Science and Technology, 2011. **8**(5): p. 051003.

27. Sucipta, M., et al., *Biomass Solid Oxide Fuel Cell-Microgas Turbine Hybrid System: Effect of Fuel Composition.* Journal of Fuel Cell Science and Technology, 2008. **5**(4): p. 041006-041006.

28. Woudstra, N., T.P. van der Stelt, and K. Hemmes, *The Thermodynamic Evaluation and Optimization of Fuel Cell Systems.* Journal of Fuel Cell Science and Technology, 2006. **3**(2): p. 155-164.

29. Bosch, K., N. Woudstra, and K. Van der Nat. *Designing solid oxide fuel cell gas turbine hybrid systems using exergy analysis*. in *The 4th International Conference on Fuel Cell Science, Engineering and Technology*. 2006.

30. Granovskii, M., I. Dincer, and M.A. Rosen, *Exergy analysis of a gas turbine cycle with steam generation for methane conversion within solid oxide fuel cells.* Journal of Fuel Cell Science and Technology, 2008. **5**(3): p. 031005-031005.

31. Leucht, F., et al., *Fuel cell system modeling for solid oxide fuel cell/gas turbine hybrid power plants, Part I: Modeling and simulation framework.* Journal of Power Sources, 2011. **196**(3): p. 1205-1215.

32. Yi, Y., et al., *Analysis and optimization of a solid oxide fuel cell and intercooled gas turbine (SOFC–ICGT) hybrid cycle.* Journal of Power Sources, 2004. **132**(1): p. 77-85.

33. Selimovic, A. and J. Palsson, *Networked solid oxide fuel cell stacks combined with a gas turbine cycle.* Journal of Power Sources, 2002. **106**(1): p. 76-82.

34. Sarmah, P. and T.K. Gogoi, *Performance comparison of SOFC integrated combined power systems with three different bottoming steam turbine cycles.* Energy Conversion and Management, 2017. **132**: p. 91-101.

35. Aravind, P.V., et al., *Thermodynamic evaluation of small-scale systems with biomass gasifiers, solid oxide fuel cells with Ni/GDC anodes and gas turbines.* Journal of Power Sources, 2009. **190**(2): p. 461-475.

36. Calise, F., et al., *Simulation and exergy analysis of a hybrid solid oxide fuel cell (SOFC)–gas turbine system.* Energy, 2006. **31**(15): p. 3278-3299.

37. Bavarsad, P.G., *Energy and exergy analysis of internal reforming solid oxide fuel cell–gas turbine hybrid system.* International Journal of Hydrogen Energy, 2007. **32**(17): p. 4591-4599.

38. Aminyavari, M., et al., *Exergetic, economic, and environmental evaluations and multi-objective optimization of an internal-reforming SOFC-gas turbine cycle coupled with a Rankine cycle.* Applied Thermal Engineering, 2016. **108**: p. 833-846.

39. Petersen, T.F., N. Houbak, and B. Elmegaard, *A zerodimensional model of a 2nd generation planar SOFC using calibrated parameters.* International Journal of Thermodynamics, 2006. **9**(4): p. 147-159.

40. Patel, H.C., T. Woudstra, and P.V. Aravind, *Thermodynamic Analysis of Solid Oxide Fuel Cell Gas Turbine Systems Operating with Various Biofuels.* Fuel Cells, 2012. **12**(6): p. 1115-1128.

41. Ozcan, H. and I. Dincer, *Performance evaluation of an SOFC based trigeneration system using various gaseous fuels from biomass gasification.* International Journal of Hydrogen Energy, 2015. **40**(24): p. 7798-7807.

42. Bicer, Y. and I. Dincer, *Energy and exergy analyses of an integrated underground coal gasification with SOFC fuel cell system for multigeneration including hydrogen production.* International Journal of Hydrogen Energy, 2015. **40**(39): p. 13323-13337.

43. O'hayre, R., et al., *Fuel cell fundamentals*. 2016: John Wiley & Sons.

44. Choi, Y., et al., *Continuum and Quantum-Chemical Modeling of Oxygen Reduction on the Cathode in a Solid Oxide Fuel Cell.* Topics in Catalysis, 2007. **46**(3): p. 386-401.

45. Istomin, S.Y. and E.V. Antipov, *Cathode materials based on perovskite-like transition metal oxides for intermediate temperature solid oxide fuel cells.* Russian Chemical Reviews, 2013. **82**(7): p. 686.

46. Saravanamuttoo, H.I.H., G.F.C. Rogers, and H. Cohen, *Gas turbine theory*. 2001: Pearson Education.

47. Kim, T., et al., *A study of carbon formation and prevention in hydrocarbon-fueled SOFC.* Journal of Power Sources, 2006. **155**(2): p. 231-238.

48. Baldinelli, A., L. Barelli, and G. Bidini, *Upgrading versus reforming: an energy and exergy analysis of two Solid Oxide Fuel Cell-based systems for a convenient biogas-to-electricity conversion.* Energy Conversion and Management, 2017. **138**: p. 360-374.

49. Bale, C., et al., *FactSage thermochemical software and databases.* Calphad, 2002. **26**(2): p. 189-228.

50. Available from: http://www.asimptote.nl/software/cycle-tempo/cycle-tempo-details/. [cited 2017 26 August];

51. Aravind, P., J. Ouweltjes, and J. Schoonman, *Diffusion impedance on nickel/gadolinia-doped ceria anodes for solid oxide fuel cells.* Journal of The Electrochemical Society, 2009. **156**(12): p. B1417-B1422.

52. Ahn, J.S., et al., *High-performance bilayered electrolyte intermediate temperature solid oxide fuel cells.* Electrochemistry Communications, 2009. **11**(7): p. 1504-1507.